Chapter 9
Lightwave synthetic noise generation

The characterization of the noise performance of lightwave receivers is of basic importance for optical communication systems. Spectral intensity measurements on noise are conveniently be made with signal generators delivering white noise with known noise levels. These methods are superior in simplicity and accuracy, compared to direct noise measurements (see section 8.1), since additional gain measurements are not required. Other methods, including direct methods, require a separated measurement of receiver gain to reconstruct the input noise from the measured output noise.
As early as 1953, the IRE recommended [817] the application of white noise generators (dispersed signal sources) in electrical noise measurements. A convenient and commercially available *lightwave* noise generator is lacking (1994), and therefore noise measurements on lightwave receivers are usually restricted to direct measurements. Recently, we proposed a lightwave synthetic noise generator for noise measurements that generates white noise currents when illuminating PIN photo diodes [802,801,803,901,902]. The proposed generator is primary intended for electrical and optical measurements of noise, however it is also applicable for transfer measurements.
In this chapter, we analyze the principles of synthetic noise generation in detail. Much effort of this thesis work was focused on the development of such a noise generator.

State of the art of lightwave based noise measurements
In the literature, various lightwave methods are described to measure noise in lightwave receivers. These methods are listed below.

- Direct noise measurements on lightwave receivers are widely used [807, 808, 809, 810, 811, 812, 813, 814, 815]. In these references receiver output noise was measured directly (usually with a spectrum analyzer), then receiver gain was measured or estimated, and the equivalent input noise was reconstructed from these quantities. These methods suffer from limited accuracy since the separated gain measurement must accurately incorporate all mismatch errors and all noise detection errors of the noise measurement.
- Shot noise methods are more convenient, since the shot noise level is known from dc measurements: $S_i=2q\cdot I_{dc}$. Kaspar et al. [805] compared the equivalent input noise of a *balanced* receiver with the white shot noise generated by a laser. The balanced configuration facilitates suppression of (unknown) laser RIN. Machida and Yamamoto [806] measured squeezing of light using a similar ratio noise measurement. They generated white shot noise in a balanced pair of photo diodes using an LED. Clean light sources, such as incandescent lamps [801], are sometimes preferred since it is assumed that they do not suffer from unknown RIN levels. All shot noise methods suffer from large dc photo currents to generate an adequate shot noise level. This may overload unbalanced receivers.

• Amplified spontaneous emission from optical amplifiers [816] may provide higher noise levels for comparative dc currents. Nevertheless, the noise power is spread out over thousands of GHz, which indicates that most noise power is unused.
• Lasers modulated with white electrical noise or lasers with high RIN provide higher noise levels. They are not white over a wide frequency band, which prevents them from a simple wideband calibration, performed at low frequencies only.
• We proposed *synthetic noise* for lightwave receiver noise measurements [801,803] and for electrical noise measurements [802]. We used the source of Wang et. al. [907], who proposed a bandwidth measurement setup, improved its spectral flatness [901,902] and calibrated it with shot noise [801]. The major advantages of synthetic noise are that:
(1) the total rms-noise current is as high as 70% of the dc photo current, and that
(2) all available noise power is concentrated in a user definable bandwidth B.

A variable noise bandwidth is an advantage to maximize noise power and to minimize spurious response. The wider the spectral width of the signal is, the more the available power is spread out over the frequency band and the lower the spectral intensity will be. A large portion of the synthetic noise band is applicable for white noise purposes, and can be as wide as twice the maximum lightwave FM sweep of the laser. Variable noise band widths up to hundreds of GHz are assumed to be feasible when multi-section lasers are applied.
All these aspects make the synthetic noise method superior to the previous methods.

State of the art of synthetic noise generation.
As early as 1953, the IRE recommended [817] the use of white noise generators (dispersed signal sources) for noise measurements. Suggested white noise sources are (1) *natural* noise generators such as noise diodes or gas tubes and (2) *synthetic* noise generators such as oscillators whose frequencies are swept through the band at a uniform rate.
Electrical synthetic noise generators are inconvenient for wide band noise measurements, since their spectral width is restricted to the maximum FM sweep of the modulated oscillator. On the other hand, the lightwave synthetic noise principle is quite applicable for the generation of wideband noisy signals. This is because a weak FM modulation at lightwave frequencies will easily cause a frequency swing of several GHz.
Wang et al. [907] proposed in 1989 a lightwave source for bandwidth measurements, using the delayed self-homodyne spectrum of a DFB laser. The delayed self-homodyne principle [903,905], and more recently the self-heterodyne [904] principle, are well-known from laser linewidth measurements [903,905]. In addition, Wang et al. modulated the laser frequency with a sinusoidal signal to spread out the homodyne spectrum over a very wide frequency band. They recommended a delay significantly larger than the coherence length of the DFB laser to smooth the output spectrum into a white noise spectrum. As a result, the Wang experiment [907] required a delay of more than 1 km fiber length.

A first prototype of this new lightwave setup, that was made available for this thesis work, was developed by van Deventer [908]. We developed novel techniques for wideband noise measurements on lightwave receivers [801,803 and section 8.4.4 and 8.3.3], using this lightwave source, and proposed the name *synthetic noise source*. We proposed this principle for a novel electrical noise source [802], and demonstrated some advantages, compared to conventional electrical sources. In addition we proposed the noise-tee [802] as discussed in section 8.2.
Next, we improved the spectral flatness of synthetic noise using electrical noise injection and triangular modulation [901,902] and we proposed multi-loop stabilization. The noise injection facilitates the use of multi section lasers. They are preferred rather than DFB lasers due to their superior FM modulation performance. Since these lasers are commonly optimized for maximal coherence, the application of noise injection makes a delay length of several kilometers superfluous. Some improvements are listed in figure 9.1.

Wang experiment	*our improvements*	*remarks*
sinusoidal FM modulation	triangular FM modulation	This improves the usable portion of the available noise bandwidth
parasitic laser noise (laser linewidth)	external noise injection	This reduces the spectral ripple. Pink noise injection is preferred to white noise injection to make efficient use of available noise power
long delay required for adequate incoherence. (1km, combined with 100kHz modulation)	short delay is adequate (e.g. 10m, combined with 10MHz modulation)	Due to noise injection. Strong incoherence improves the spectral ripple, and noise relaxes the incoherence requirements such as delay length. A short delay length simplifies practical implementation.
DFB laser. Linewidth of 20 MHz or more is essential for good performance	multi section lasers are also feasible, linewidth is irrelevant	Due to short delay. Multi section lasers are superior in FM performance. This facilitates huge noise bandwidths
unstabilized	multi-loop methods for stabilization of noise intensity spectrum	Independent stabilization of optical power and noise intensity spectrum

Fig 9.1 *Overview of various improvements that made a simple reproduction of the synthetic noise source viable.*

Highlights of this chapter
The highlights of this chapter, which are developed during the work on this thesis, are:
- Development of a novel lightwave device, a *synthetic noise generator* that provides white noise when it illuminates PIN photo diodes.
- *Improvements* to lightwave synthetic noise generation, using noise injection and triangular modulation [901: patent pending, 902].

- Dual loop method, for independent *stabilization* of the synthetic noise level as well as the optical power of synthetic noise generators [901: patent pending].
- Detailed *analysis* of many practical and theoretical aspects of synthetic noise generation.
- Practical implementation of a synthetic noise generator to demonstrate the feasibility of the proposed methods.

9.1. Basic principles of synthetic noise generation

A lightwave synthetic noise generator is an FM modulated laser, of which the lightwave spectrum is down converted into the 'electrical' frequency band. It uses the delayed self-homodyne principle for down conversion.
This introductory section describes the basic ideas behind synthetic noise generation, and demonstrates the feasibility and performance of this new noise source. The backgrounds are analyzed in section 9.2 from a practical point of view, and in section 9.3 from a theoretical point of view.

9.1.1. Delayed self-homodyne principle with FM modulation

The lightwave synthetic noise source starts from a laser source, of which the lightwave output is modulated in frequency. The block diagram in figure 9.2 presents this by means of an electrical source that generates a periodic signal with frequency f_m, such as a 10 MHz sinusoidal or triangular signal. The modulation is deep enough to modulate the lightwave frequency over several giga-Hertz.

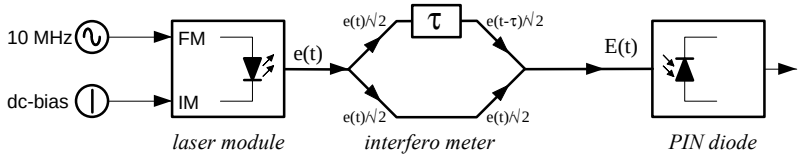

Fig 9.2 *Block diagram of the synthetic noise generator. The modulation frequency modulates the lightwave frequency. The delay in the interfero-meter causes two lightwave FM-signals, that differ in frequency. The PIN-diode performs the duties of a down converting mixer, to generate an electrical differential frequency that sweeps periodically at modulation rate.*

The use of a noise-free laser would have led to a modulated lightwave spectrum with discrete equidistant frequencies (see figure 9.3). The difference in frequency between each frequency component and the lightwave carrier is exactly a multiple of the modulation frequency f_m.

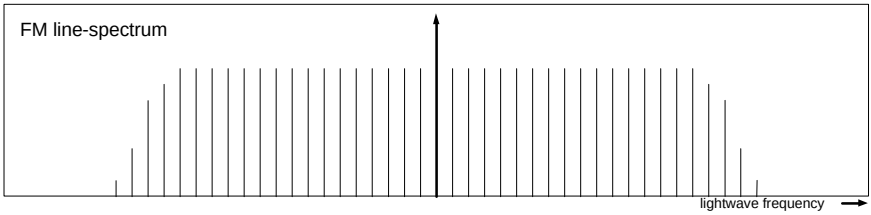

Fig 9.3 *The laser output (FM) spectrum is essentially a line spectrum, with equidistant lines. This is a simplified picture; in practice the spectrum is generally not flat as is shown in figure 9.10.*

The linewidth of practical lasers prevents the lightwave spectrum from being a perfect line spectrum. As a result, a lightwave spectrum analyzer with very high resolution will indicate a comb spectrum that is similar to the spectrum in figure 9.5a.

Next, the lightwave signal is split, one beam is delayed and both beams are combined by means of a fiber optic interferometer. The difference in length between the two optical branches ranges from a few meters to many kilometers, in practical setups.
The composite lightwave signal is essentially the composition of two FM modulated lightwave signals. Under optimal delay conditions, which are discussed in a little while, the momentaneous frequencies oscillate symmetrically around a common mean value (see figure 9.4). The frequency sweep depends on the FM modulation depth.

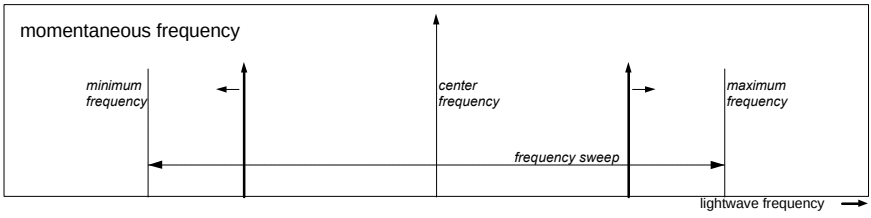

Fig 9.4 *The output signal of the synthetic noise generator is essentially the composition of two FM modulated lightwave signals, of which the momentaneous frequencies oscillate symmetrically around a common mean value.*

The composed lightwave signal illuminates the PIN photo diode. This diode performs the duties of a down converting mixer, because of its linear *power* response. Since this is similar to a *quadratic* field strength response, the non-linear transfer converts the two optic frequencies into components with other frequencies. The sum and differential frequency are included.
DC-currents and currents with the differential frequency are the principal currents that escape from the electrical passband of the diode[1]. All other converted components have frequencies in the lightwave range and are therefore unable to escape from the PIN diode chip as electrical current.

[1] Note that spurious AM and shotnoise also cause minor contributions to the diode current.

The momentaneous frequency of the generated photo current equals the difference in lightwave frequency of the two lightwave signals. This difference changes periodically at the rate of the modulation frequency f_m, which causes the momentaneous frequency to change at the same rate. The maximum momentaneous frequency of the photo current equals the maximum frequency difference, which can be as high as twice the modulation depth. As a result, a weak modulation in frequency of the lightwave signal causes a giant absolute change in frequency of the photo current.
The concept of momentaneous frequency is adequate for a time-domain description, however, frequency domain descriptions require Fourier series. Since the modulation frequency of practical synthetic noise generators is 100 kHz or more, a spectrum analyzer is unable to track these rapid frequency changes. As a result, they will display the Fourier components of the photo current, with many equidistant frequencies. The detected spectrum is similar to the spectrum in figure 9.3, with the center frequency at zero Hz.

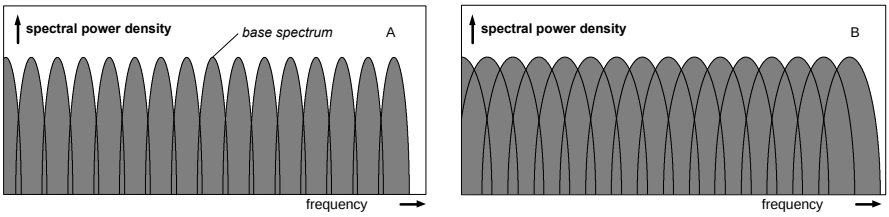

Fig 9.5 *The output (FM) spectrum of the synthetic noise generator is essentially a line spectrum, with equidistant lines. The phase noise (linewidth) of each line fades the discrete spectrum into a continuous spectrum. The envelope ripple of spectrum (a) is deeper than that of spectrum (b) because the width of the individual lines in (b) is wider. The wider the linewidth is, the more a white noise spectrum is imitated.*

The non-zero linewidth of practical lasers causes a spectrum with broaden lines as shown in figure 9.5a. From now on, we call this a comb spectrum.
The wider the laser linewidth, the wider all comb lines will be (see figure 9.5b), and the better the comb spectrum is converted into a flat spectrum with weak ripple. In a well-designed synthetic noise generator, this spectral ripple is very small. As a result, spectrum analyzers display a white spectrum, and are unable to distinct synthetic noise from random white noise.

Optimal delay time
The choice of this differential delay τ and of the modulation frequency f_m is inter-related. When $f_m=1/(2\tau)$, then the two lightwave signals are 180° out of phase at when the two signals are combined. The lightwave frequencies oscillate symmetrically around a common mean value and the frequency sweep of the differential frequency becomes maximal. This is one of the reasons why this choice is an optimal choice.
Another reason to choose this value, is associated with suppression of parasitic IM modulation. The unwanted IM components in the lightwave signal interfere with the down-converted FM signal and infect the 'white' spectrum with equidistant spikes at a

multiple of the modulation frequency. When the lightwave signals in both branches are perfectly 180° out of phase, then full extinction of parasitic IM components will result. It will optimally suppress the odd harmonics of the IM signal in the photo current.
In conclusion:

$$\boxed{f_m=1/(2\tau)} \qquad \textit{results in}: \begin{cases} \text{maximum frequency sweep} \\ \text{optimal IM suppression} \end{cases}$$

We observed in our experimental setup that optimal IM suppression did not coincide with the above condition. It is plausible that this originates from small unbalance in the interferometer. In a practical setup, it is useful to de-tune the modulation frequency to improve the IM suppression.

Definitions
We summarize now some useful definitions, to simplify the description of synthetic noise generation.

- The *lightwave synthetic noise generator* is the lightwave device of figure 9.2, excluding the PIN-diode. Its output is the lightwave output of the interfero meter. This PIN-diode can be any arbitrary diode, including the input diode of an optical receiver under test [801] or a lightwave noise-tee [802]. Therefore, this PIN diode is no part of the generator itself.
- The *synthetic noise spectrum* is the response spectrum of the photo current that flows through a PIN diode when illuminated by the lightwave noise source.
- The *homodyne spectrum* is the synthetic noise spectrum, when the periodical modulation is switched off.
- The *frame* of the synthetic noise spectrum is a discrete line spectrum that would have occurred when a perfect laser (with zero linewidth) is used. The elements of a frame are *frame lines* and have zero linewidth.
- The *comb* of the synthetic noise spectrum is the set of all individual spectra that are drawn in figure 9.5. The elements are *comb lines* and have a non-zero linewidth. The addition of all comb lines yields the synthetic noise spectrum.

9.1.2. Example of a practical synthetic noise generator

To demonstrate the feasibility and the performance of practical synthetic noise generators, we constructed an experimental setup with a DFB laser (1530 nm, 60 dB optical isolator), a fiber optic interferometer (about ΔL=10 m differential delay, manual polarization adjustment) and a 10 MHz function generator. A block diagram of this setup is shown in figure 9.6.
The laser diode was modulated[2] in frequency (FM) by weak modulation of its bias current. This way of modulation, however, performs FM modulation as well as intensity modulation (IM). This IM effect is of minor importance since the process of FM to IM conversion in the interferometer largely dominates the parasitic IM modulation.

[2] In this experiment, triangular modulation and noise injection was used, as discussed in the succeeding sections.

The lightwave output signal was detected with a low noise optical receiver and a spectrum analyzer (HP8566b). The measured spectra were extracted by a computer to perform post processing of data. The detected dc photo-current was 100 μA.

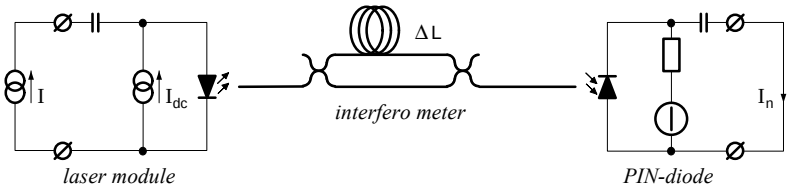

Fig 9.6 *Block diagram of an implementation model of the lightwave synthetic noise generator. The current I represents the periodic modulation current, and I_{dc} represents the bias current.*

Measurement and post processing. First, the synthetic noise spectrum was detected for various amplitudes of the 10 MHz signal. In addition, the system noise of the measurement system was detected by detecting the output noise when the illumination is removed from the optical receiver.
All these raw spectra are distorted by the unknown gain profile of the optical receiver and the unknown contribution of the noise by the measurement system. Therefore, the system noise was removed from the raw data, by subtraction of spectra on a power base. When U is the voltage that is detected with a selective voltmeter (spectrum analyzer), and when U_x and U_0 are the voltages that are associated with an illuminated and a non-illuminated receiver respectively, then the noise correction is performed with: $U'_x = \sqrt{(U_x^2 - U_0^2)}$.
Subsequently, the gain profile is reconstructed from the measured spectra by the assumption of a perfect white spectrum. To perform this, spikes, dips and weak fluctuations are stripped by proper interpolation and averaging techniques. When G is the smoothed function resulting from the spectrum originated from the deepest modulation, then the gain correction of all spectra is performed with U" = U' / G.

Observations. Figure 9.7 demonstrates the post-processed noise spectra, for various modulation depths. The maximum modulation current, that was used in the experiment, is denoted with I_m. Its rms-value was about 12% of the laser bias current (60mA bias) to preserve linear FM modulation of the laser.
The spectral width is proportional to the maximum lightwave differential frequency, that is proportional to the amplitude of the modulation current I. The spectral width of the spectrum that originates from the modulation current $I_m/16$ is about 650 MHz. From this observation it is concluded that modulation with I_m will cause a spectral width that is 16 times wider, which is more than 10 GHz.
According to section 9.2.3 and 9.3.2, the rms-magnitude of the synthetic noise is independent of the modulation depth. As a result, the product of noise bandwidth and spectral intensity is invariant, which makes this density reciprocal to that current. Figure

9.7 shows that doubling the modulation depth results in 3 dB decrease of spectral intensity of the noise current.

The reconstructed spectra, that originate from modulation with the magnitudes $I_m/2$ and $I_m/4$, are perfectly white. From the precision that is associated with these spectra, it is concluded that the performed post processing is correct and accurate.
The reconstructed spectrum, that originates from modulation with the magnitude $I_m/8$, bears a slight deviation from white noise. The predicted spectral width is 1300 MHz for this current. From this weak deviation, and this prediction, it is concluded that approximately 50% of the synthetic noise spectrum is applicable for measurement purposes with white noise.

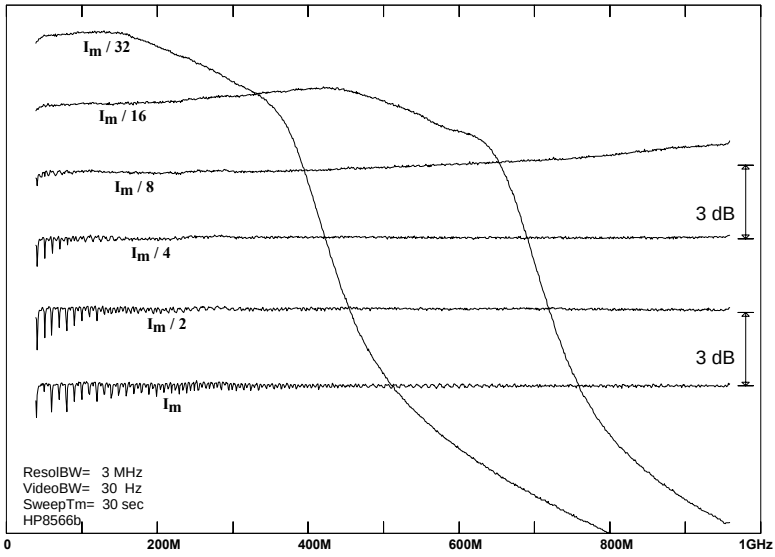

Fig 9.7 *Measured output spectrum of a well-designed synthetic noise generator, for various modulation currents. All modulation currents are related to an arbitrary maximum value I_m. Its rms-value was about 12% of the laser bias current (60mA). Doubling the modulation depth resulted in twice the noise bandwidth and 3 dB decrease of spectral noise density. Note that triangular modulation and noise injection was performed as discussed in section 9.2.*

Practical aspects. The small dips at the low end of the spectra in figure 9.7 originate from parasitic intensity modulation of the laser. The wider the spectrum, the deeper the modulation is required and the more the dips are pronounced in the spectrum. The use of a modern multi section laser, with separate inputs for IM and FM modulation, will probably nullify these side effects.
The maximum obtainable spectrum width is device dependent. A DFB laser, such as is used in this experiment, is not intended for frequency modulation. Its choice is therefore

not optimal. The use of modern multi section lasers will probably facilitate a spectrum width of 100 GHz or more.

9.1.3. Conclusions

In conclusion, we described the basic principles of a novel lightwave device, a synthetic noise generator. The instrument was original introduced as an alternative for bandwidth measurements, however we extended its applicability to lightwave noise measurements. We implemented an experimental setup, using a DFB laser diode, 10 MHz modulation and 10 m differential delay. We demonstrated that the experimental setup is usable up to 10 GHz. Multi section lasers may increase this band width to hundreds of GHz.

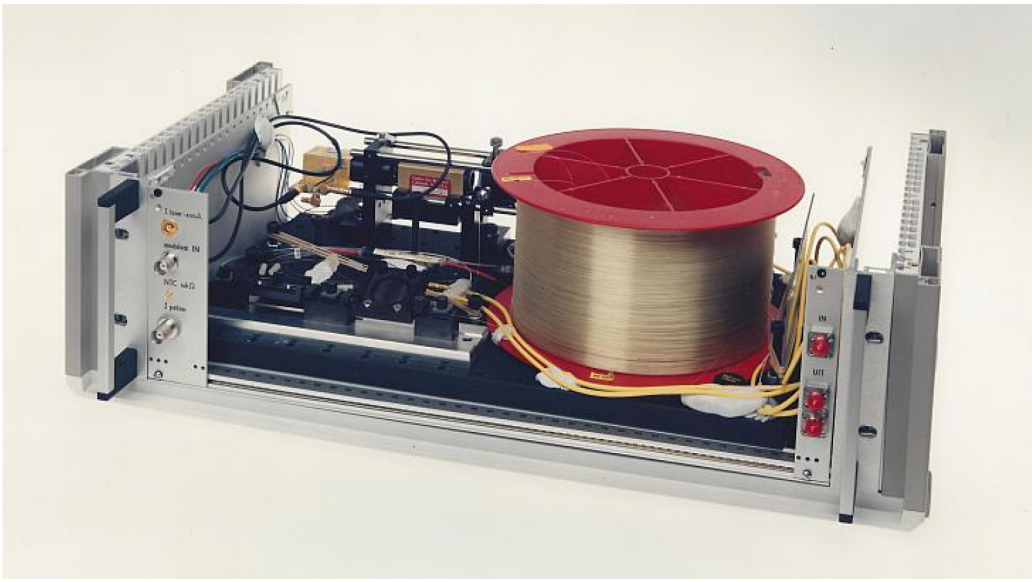

Fig 9.x Implementation of the lightwave synthetic noise generator, based on the diagram in fig 9.6.

9.2. Practical analysis of synthetic noise generation

The previous section was focused on a general understanding of synthetic noise generation, by discussing basic principles and the results from experiments and simulations. This section will focus on deeper understanding, and analyzes the principles of synthetic noise generation from a practical point of view. It uses the mathematical results from the theoretical analysis, as is described in section 9.3.

9.2.1. Analysis of the spectral envelope of the synthetic noise

The flat spectra in figure 9.7 have demonstrated that the spectral ripple in the synthetic noise spectrum can be made very small. So far, it was assumed that all ripple is caused by the distance between the individual comb lines in the spectrum. Unfortunately, this is not true. This subsection will demonstrate that the frame of the synthetic noise spectrum has a bumpy envelope, and that property dominates in the spectral ripple.

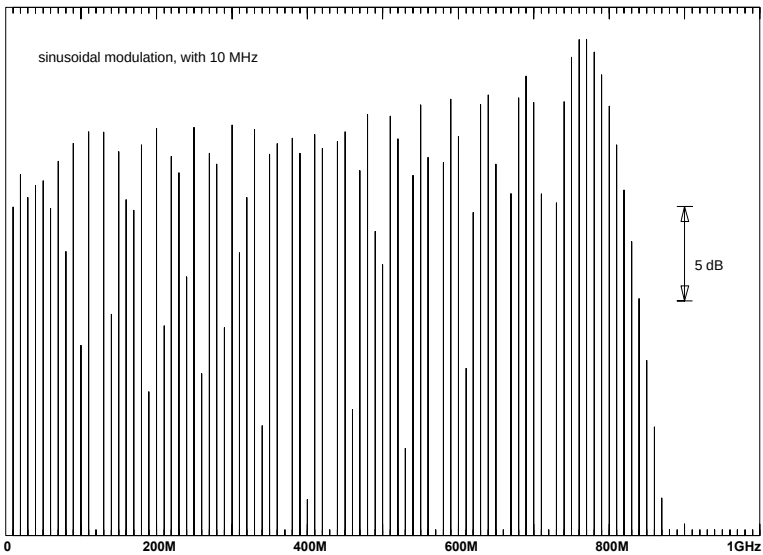

Fig 9.8 *Simulated frame of the synthetic noise. This line spectrum originated from sinusoidal modulation. A fiber length of about 10 m is required to realize an optimal differential delay for 10 MHz modulation.*

Figure 9.8 shows the simulation of a frame of the synthetic noise spectrum, in case of sinusoidal modulation. It is based on the theory of the succeeding section 9.3.3. The Bessel functions of figure 9.8 demonstrate that the frame envelope is quite rugged. Variations of more than 20 dB are observed for the intensity of succeeding frame lines.
The simulation has further demonstrated that a weak change in modulation depth results in a significant variation of this envelope. The location and periodicity of the variations in the spectral envelope change with the modulation depth. As a result, the width of each comb line must span several frame lines to eliminate spectral ripple.

Another aspect that is observed from figure 9.8, is the increase with frequency of the mean envelope curve. Its deviation from a constant value prevents the synthetic noise spectrum from being usable as *white* noise over the full power bandwidth.
Wang et.al. [907] restricted their experiments to sinusoidal modulation only. They identified the problem of this deviation, derived an approximation for the mean envelope curve, however they did not find a solution. This work has resulted in a significant improvement to synthetic noise generation by using *triangular* modulation in stead of sinusoidal modulation.
Figure 9.9 shows the simulation of a frame of the synthetic noise spectrum under triangular modulation. It demonstrates that the mean envelope curve is significantly improved, compared to its equivalent in figure 9.8. The intensity variations of the individual frame lines are comparative in both figures, however the mean envelope curve in figure 9.9 is more constant over a wide frequency interval. Figure 9.10 is even more convincing.

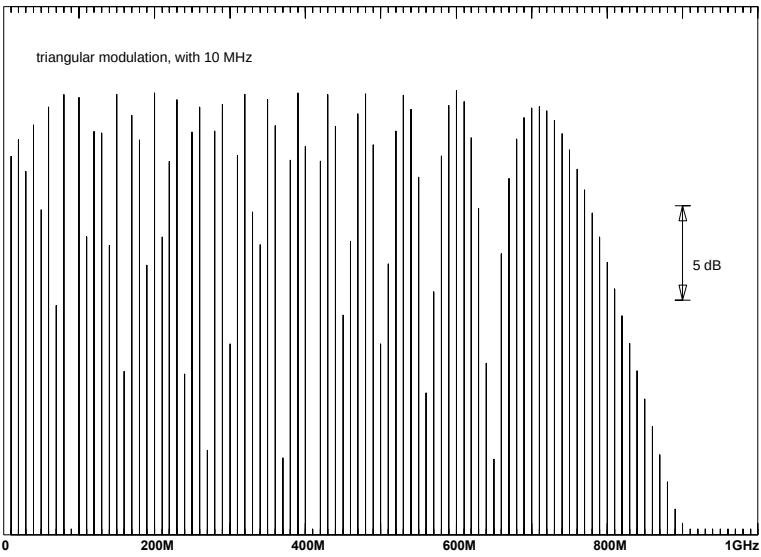

Fig 9.9 *Simulated frame of the synthetic noise. This line spectrum originated from triangular modulation. A fiber length of about 10 m is required to realize an optimal differential delay for 10 MHz modulation.*

As was stated before, the width of each comb line must span several frame lines to facilitate a smoothed synthetic noise spectrum. The more frame lines that are packed within the width of a comb line, the smaller the ripple will be in the synthetic noise spectrum. Further, the lower the modulation frequency f_m is chosen, the more tight the frame lines are packed. As a result, the lower the modulation frequency, the flatter the synthetic noise spectrum will be.
Figure 9.10 shows a simulation of the frame of a synthetic noise spectrum under triangular modulation, in which the modulation frequency is lower than in figure 9.9. It

demonstrates that the average frame envelope improves to that of the previous figure, and that the linewidth requirements of the laser are relaxed.

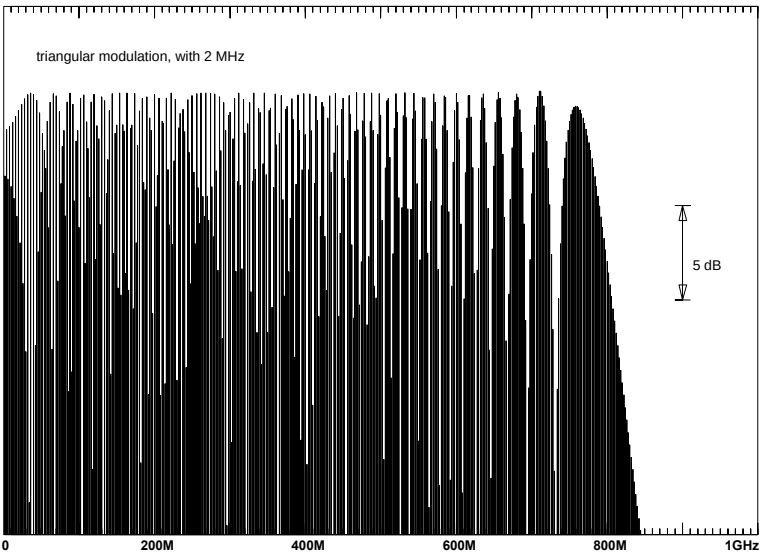

Fig 9.10 *Simulated frame of the synthetic noise. This line spectrum originated from triangular. A fiber length of about 50 m is required to realize an optimal differential delay for 2 MHz modulation.*

The draw-back of a decrease in modulation frequency f_m is the increase of differential length that the interfero meter requires for an optimal match to f_m. A length of more than 10 kilometers is assumed to be unacceptable for a viable implementation, which sets a lower limit to the modulation frequency (f_m > 10 kHz). As a result, the lower the modulation frequency, the less viable the synthetic noise generator will be.

Figure 9.11 shows the measured synthetic noise spectrum of a deliberate poor-designed synthetic noise generator. The ripple in this synthetic noise spectrum demonstrates that the laser linewidth is too small for the chosen modulation frequency. The significant difference between ripple periodicity and modulation frequency demonstrates that the bumps in the frame envelope dominate in the spectral ripple.
As expected from the previous analysis, the experiment confirmed that the location and periodicity of the spectral ripple changes with the magnitude and the wave form of the modulation signal. Similar results were obtained from extended simulations that considered the envelope of the individual comb lines.
Another aspect that is confirmed by this experiment is that triangular modulation improves the mean spectrum. As was discussed before, the dips and spikes below 200 MHz result from the parasitic intensity modulation.

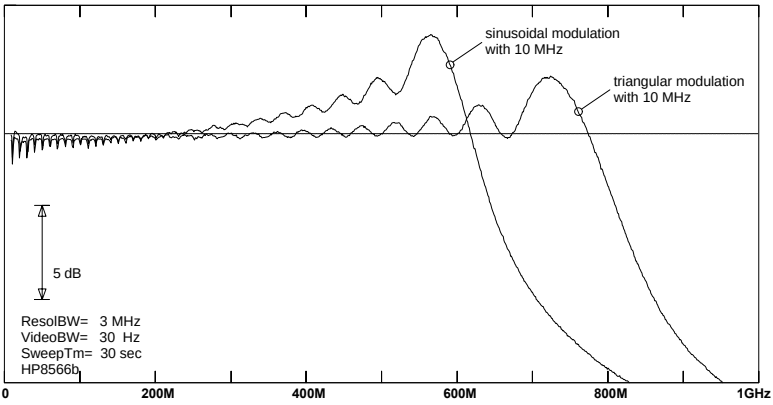

Fig 9.11 *Measured output spectrum of the synthetic noise source, to demonstrate the ripple in the envelope of the FM line-spectrum. This ripple illustrates that the differential delay in the interfero meter is too short with respect to the coherence length of the laser. Both spectra oscillate around an average that increases with frequency, however triangular modulation minimizes the inclination of this average.*
The rms-value of the periodical modulation current was approximately 0.8% of the laser bias current (60mA). Noise was not injected.

9.2.2. Spectral ripple reduction by noise injection

A ripple in the synthetic noise spectrum, that is as high as in figure 9.11, is unacceptable for noise measurement purposes. Wang et al. [907] kept this ripple as low as possible by choosing the differential delay τ in the interferometer significantly larger than the coherence time τ_c of the DFB laser. They implemented a delay with 1 km fiber, which facilitated that the optimal modulation frequency is relative low (100kHz). As a result, the comb lines are tighter packed than in figure 9.11, and the spectrum is more evenly smoothed by the laser linewidth (note the difference in envelope of the line spectra in figure 9.9 and 9.10).

The basic drawback of this approach is the delay line of more than 1 km fiber to fulfill these incoherence requirements. It will exclude the application of multi section lasers. These lasers are commonly optimized for minimum linewidth (maximum coherence length), and the use of these lasers would then require a delay line of even more kilometers.
We found a novel solution [901,902] to this discrepancy. We proposed broadening the linewidth of the individual comb lines in stead of tighter packing. An artificial increase of the laser linewidth (equivalent with a decrease in coherence length) will broaden the width of the comb lines and will improve the smoothing of the synthetic noise spectrum. As a result, tighter packing of the comb lines becomes superfluous, and the application of relative high modulation frequencies and relative short delay lengths becomes adequate (e.g. 10 m and 10 MHz).

Basic principle

The idea of noise injection is based on the understanding that an additional FM modulation of the laser frequency with noise yields an artificial increase of its linewidth [909]. The random FM modulation results in lightwave frequency jittering, and this jitter manifests as a virtual increase of the laser linewidth.
The frequency jitter affects the laser frequency, the lightwave differential frequency and the comb lines in the down converted spectrum. The overall result is a synthetic noise spectrum with smoothed ripple.
Figure 9.12 shows the basic principle. A random noise signal is added to the periodic modulation signal, and the composed signal is used to modulate the laser frequency.

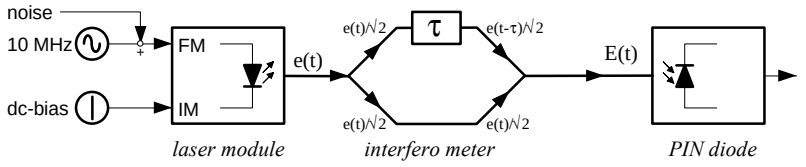

Fig 9.12 *Block diagram of the synthetic noise generator, with additional noise injection. The electrical noise current is added to the periodical modulation current, to perform an additional random FM modulation. This results in an additional frequency jitter and performs an artificial increase of the laser linewidth.*

Experimental verification
To demonstrate the impact of noise injection, we generated electrical noise. The spectral intensity was concentrated at relative low frequencies. Figure 9.13 shows the pink noise spectrum that was used for noise injection. This noise was superposed on the periodical modulation signal that generated figure 9.11. The injection level was set to approximately 7% (rms-value) of the laser bias current (60mA).

Noise injection with this relatively high injection level increases the laser linewidth significantly. Figure 9.14 demonstrates how the synthetic noise spectrum of figure 9.11 is smoothed by the proposed noise injection. The spectral ripple is vanished and the spectral width is equally increased with the linewidth.

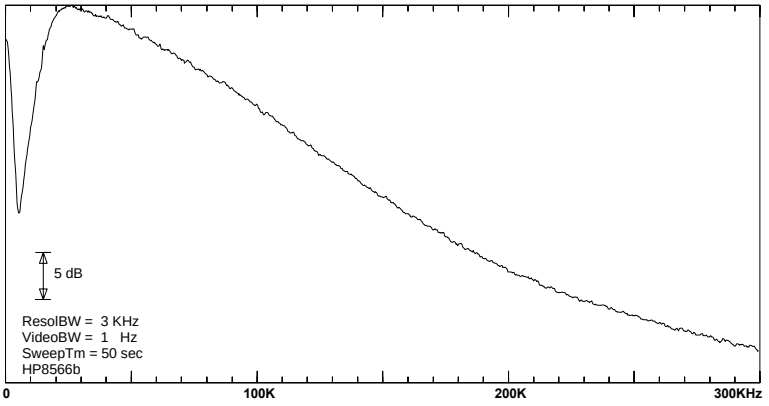

Fig 9.13 *Measured spectrum of the pink noise that was injected in the synthetic noise generator.*

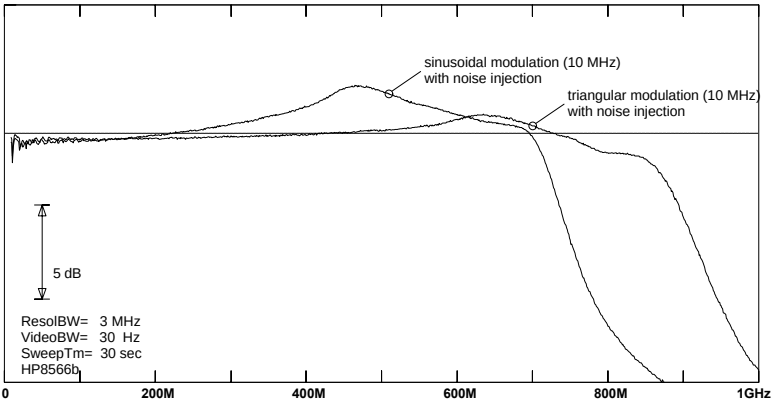

Fig 9.14 *Measured output spectrum of the synthetic noise source, to demonstrate that noise injection smoothes the ripple in the synthetic noise spectrum.*
The rms-value of the periodical modulation current was approximately 0.8% of the laser bias current (60mA). The injected noise level was approximately 7% of that bias current. This level was that high because the differential delay of the interfero meter was optimized to the 10 MHz modulation frequency and not for the spectrum in figure 9.13.

Spectrum of the injected noise

In the experimental verification we used pink noise, in stead of white noise, for noise injection. This is because we observed that the flatness of the laser linewidth curve improves when white noise injection is replaced by pink noise injection. To get a deeper understanding of this effect, we discuss the origin and shape of the laser linewidth in more detail.

Linewidth envelope: The intensity spectrum of a laser beam has essentially the well-known Lorentzian shape. When such a laser beam is detected with an appropriate delayed self-homodyne or self-heterodyne setup[3], this shape is preserved in the responding spectrum. The width of the electrical response spectrum is twice the optical laser field (see Yariv [910, page 391]).
We will refer to that response spectrum as the *homodyne noise spectrum*. It equals the synthetic noise spectrum when the periodic modulation is switched off. As a result, the homodyne noise spectrum is Lorentzian, and its shape has the following well-known form: $S = S_0 / (1+(f/\Delta f)^2) = S_0 / \left| 1+j\, f/\Delta f \right|^2$.
From a mathematical point of view, the homodyne noise spectrum is equivalent with the spectrum of a white noise source, filtered by a first order low-pass filter.

Linewidth model: The laser linewidth originates from spontaneous emission, and in addition from random electrical fluctuation such as shot noise. An adequate circuit, modeling this process, originates from a hypothetical zero linewidth laser and an intrinsic *white* noise source. The intrinsic noise source modulates the laser frequency and the resulting frequency fluctuations come through as linewidth (phase noise).
Shot noise, associated with the laser bias current, is one of the white noise currents that contributes to this intrinsic noise source. When the laser sensitivity for FM-modulation is known, then the rms-magnitude of this shot noise is indicative for the *minimum* linewidth that is expected for this laser. In practical lasers, the linewidth is significantly higher than expected from this assumption, which makes the equivalent noise source higher than the shot noise (see Henry [906] and Yariv [910, chapter 10]: linewidth enhancement factor α).

Linewidth envelope, using white noise injection: The natural linewidth of lasers virtually originates from FM modulation with internal white noise sources and has a Lorentzian shape. FM modulation of the laser frequency with *external* white noise sources yields an identical shape. Nevertheless, it will increase the laser linewidth, and thus the spectral width of the homodyne noise spectrum.
As a result, the homodyne noise spectrum with white noise injection has a first order fall-off, of which the –3 dB corner frequency marks the value of the laser linewidth. Above that corner frequency, the homodyne spectrum decreases with 6 dB per octave.

Linewidth envelope, using pink noise injection: Modulation of the laser frequency with *pink* noise will change both the width and the shape of the homodyne noise spectrum. We measured this modified shape of the homodyne noise spectrum using injection of pink noise with the spectrum of figure 9.13.
Figure 9.15 demonstrates these changes for various injection levels. It shows the synthetic noise spectrum when the periodical modulation is switched off (homodyne noise spectrum). At maximum injection level (7% of bias current), the spectrum is

[3] Some authors use the word self-heterodyning while others use self-homodyning for the same subject. This thesis reserves the word self-heterodyning for setups that are similar to self-homodyne setups, but in which one beam is additionally shifted in frequency (e.g. 100 MHz with an acousto-optic modulator). In a delayed self-homodyne setup, two beams that originate from the same light source illuminate simultaneously a PIN diode. Since one beam is delayed, the two beams will incoherently mix in the photo diode to produce the differential spectrum. Both homodyne and heterodyne setups respond with similar spectra but with different center frequency. Self-heterodyning is more complex, but avoids dc-problems caused by optical fluctuations.

observed to be flat, up to 170 MHz. Above that corner frequency, the spectrum decreases with about 12 dB/oct. The more the injected noise is attenuated, the less the width and decay will be. When all noise injection is switched off, the homodyne spectrum becomes Lorentzian with a –3 dB corner frequency at about 17 MHz.
As a result, the homodyne noise spectrum with pink noise injection has a second order fall-off. The homodyne noise spectra in figure 9.15 are similar to that of filtered white noise, that is filtered by second-order low-pass filters. Fair results were obtained with empirical curve fits, that originates from low-pass filters with one zero and two poles.

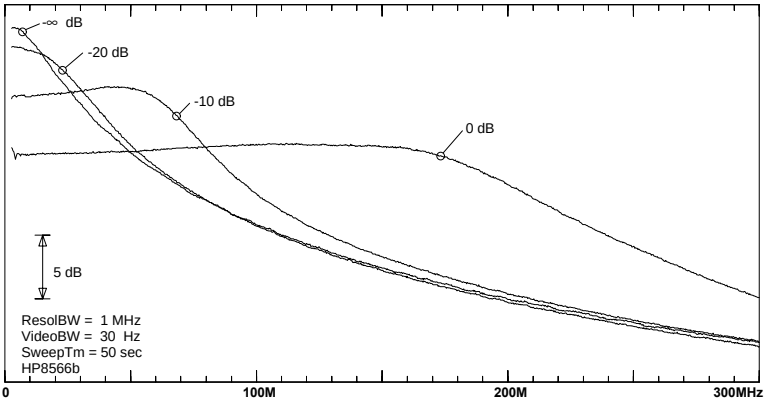

Fig 9.15 *Measured synthetic noise spectrum in case the periodical modulation of the synthetic noise generator is switched off (homodyne noise spectrum). The level of the pink noise injection (see figure 9.13) is varied in 10 dB steps. These plots demonstrate that pink noise injection increases the homodyne spectral width and modifies its shape. Filtering of the injected noise has improved the flatness of the homodyne spectrum.*

Benefits of pink noise injection: The use of pink noise injection, in stead of white noise injection, improves the smoothing 'efficiency' in the synthetic noise spectrum. This is because pink noise injection modifies the profile of the individual comb lines into a more 'rectangular' shape. As a result, the smoothing process between two succeeding comb lines is improved, and the spectral fall-off above the highest significant comb line is more abrupt. This makes the overall synthetic noise spectrum more 'rectangular' and the available noise power is more efficient concentrated within the user defined spectral width.

Simulation of homodyne spectra
The above mentioned experiments were restricted to variation of injection levels. The shape of the injected pink noise spectrum was not changed. Nevertheless, the spectral shape of this pink noise spectrum affects the homodyne spectrum too.
We did not experience with other noise spectra to inject, however we restricted these investigations to computer simulations. From these simulations, it was concluded that the shape of the injected noise spectrum is of minor importance, however the corner frequency of this low-pass profile is the most important figure of merit.

We simulated a delayed self-homodyne setup, using the time domain relations of section 9.3.1. The modulation frequency was set to f_m=10 MHz and the associated optimal differential delay was set to $\tau=1/(2\cdot f_m)$. The injection noise signal was modeled by $15\cdot10^6$ Gaussian distributed random numbers. The pink noise spectrum was simulated, using a model of three cascaded first order filters with identical corner frequency. The homodyne spectrum was calculated using standard FFT techniques[4]. The injection magnitude of each simulation was adjusted to a value that facilitates equal output density at zero Hertz.
Figure 9.16 shows the simulated results for these $15\cdot10^6$ samples. The homodyne spectrum that originates from the 10 GHz filter (∞) has a Lorentzian shape, because it originates from injected noise that is nearly white. Filtering at 1 MHz changes the shape in a way that is more close to a rectangular profile. Further reduction of this corner frequency has no more than a minor effect to the shape.

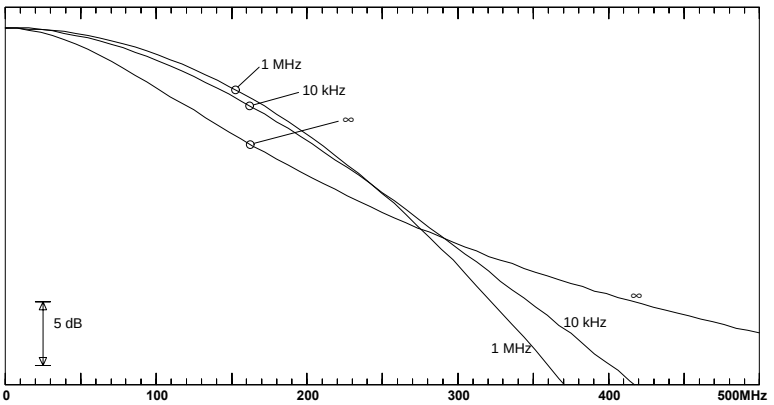

Fig 9.16 *Simulated homodyne spectrum that results from pink noise injection, for various filter corner frequencies. The injected magnitude of each simulation was adjusted to facilitate equal output density at zero Hertz.*

Similar simulations were performed at constant corner frequency of 1 MHz, however with reduced filter order. A noticeable change of shape was not observed. Other spectral adjustments to the injected noise will probably not result in a significant improvement of the homodyne spectrum, however forms an aspect of further research.

Optimal pink noise spectrum
From these computer simulations it is concluded that the filter corner frequency must be equal or lower than modulation frequency for which the synthetic noise generator is optimized. On the other hand, the lower the filter corner frequency is chosen, the more the two lightwave frequencies in the interfero meter change with equal phase and, the

[4] A single FFT calculation over $15\cdot10^6$ numbers was avoided using 450 individual FFT calculations over 32768 samples and combining these intermediate results.

lower the differential frequency will be. As a result, a higher injection level is required to preserve the spectral width of the comb lines in the synthetic noise spectrum.
From this, it is plausible that optimal noise injection is associated with a filter corner frequency that is close to the modulation frequency. Note that this conclusion is *not* verified experimentally!

9.2.3. Power analysis of synthetic noise

A fair estimation of noise power can be obtained from simple dc current measurements. Furthermore a fair estimation of spectral noise density can be made from additional measurement on spectral bandwidth. These estimations provide simple means for rough exploratory measurement of absolute noise levels, without preceding calibration of the synthetic noise source. In this subsection we discuss their relation.

When a PIN photo diode is illuminated by the synthetic noise generator, then a photo current is generated. This photo current is the superposition of the (ac) synthetic noise and a dc-current. Two characteristic aspects of this photo current can be determined simply: mean value and spectral width. The mean value I_{n0} is obtained by measurement with a pica-ampere meter, and the spectral width B by measurement with a spectrum analyzer.
The mean value I_{n0} is a constant that depends on the chosen laser, its bias current and the attenuation in the optical path. Variation of the modulation depth will not affect this value. The spectral width B is a variable that is linear proportional to the modulation depth. When B is too wide for direct measurement with the used spectrum analyzer, then it must be derived from scaled measurements. In that case, extract B' from an equivalent measurement with reduced modulation, and scale B' to B with the used modulation reduction.

The synthetic noise originates from an incoherent mix of two lightwave signals. When the interference between these two signals varies from perfect extinction to perfect superposition, then the generated photo current varies from zero to a fixed maximum value. As a result, the photo current is a random current with rapid variations from zero to twice a mean value I_{n0}.
Under these conditions, the relation between the mean value and the rms-value of the ac current $i_n(t)$ can be evaluated simply (see section 9.3.2). Further, the relation between rms-value and spectral density S_i can be evaluated simply when the spectral width B is known. The product of S_i and B equals the square of the rms-value, according to the Parceval identity for spectra. For these quantities, we obtain:

I_{n0}	= *generated dc current*
$i_{rms} = I_{n0}/\sqrt{2}$	= *rms-magnitude of the noise*
$S_i(f) \approx \left(I_{n0}/\sqrt{2B} \right)^2$	= *spectral intensity*
$\mu \stackrel{\text{def}}{=} (\sqrt{S_i})/I_{n0} \approx 1/\sqrt{(2 \cdot B)}$	= *noise-current ratio*

These expressions quantify how extremely efficient a synthetic noise generator is. Up to 70% of the generated dc-current is also available as noise. When this synthetic noise is

equally spread out over a full frequency band of B=50 GHz, and I_{n0}=100μA dc-current flows through the photo diode, then the spectral noise density will be as high as 316 pA/√Hz. This is 25 dB more than the thermal noise current of a 50Ω resistor. A dc-current of more than 300 mA would have been required to generate an equal spectral intensity by means of shot noise.
The definition of the noise-current ratio μ is similar to the well-known laser-RIN definition. In this example its value in [dB/Hz] is: $10 \cdot \log_{10}(\mu^2) = -110$ [dB/Hz]. This level is more than 40dB higher than typical RIN specifications for laser diodes. It illustrates that the ignorance of laser RIN effects does not vitiate our analysis.
From figure 9.7 it is observed that about 50% of the spectral width B is applicable for noise measurement, which is 25 GHz in this example.

For accurate scaling purposes, it is required that both I_{n0} and S_i are stable quantities. This is because ratio measurements require a precise variation of S_i. which is monitored by measuring the variation of the dc-current I_{n0}. Improvement of the individual components does not yield the required stability. Stabilization of the laser output power, the laser temperature and its modulation current is a commonly used measure. Further improvement of the individual components would require additional measures, such as stabilization of polarization drift in the interferometer, which makes it an inconvenient approach.
This work has resulted in novel techniques [901], to stabilize S_i by controlling the magnitude of the modulation current. This novelty is based on the understanding that an increase of the modulation depth will *increase* the spectral width B however will *decrease* the spectral density S_i. Figure 9.17 demonstrates the basic principle in which an additional control loop is used to stabilize I_{n0} simultaneously.

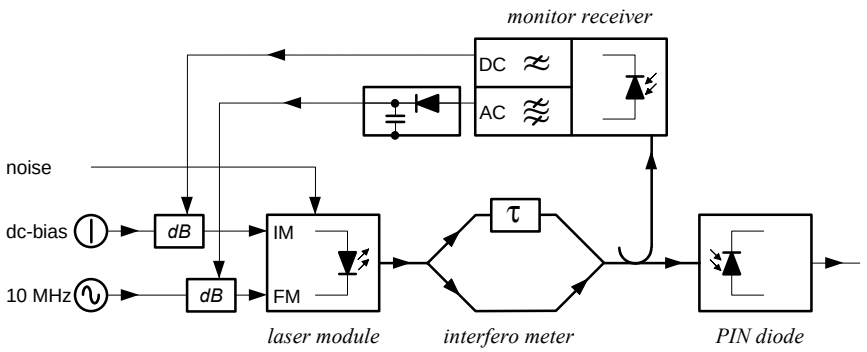

Fig 9.17 *Dual loop method to stabilize the optical power as well as the intensity spectrum of the synthetic noise current. Both quantities are independently controlled.*

The control loop monitors the output signal of the synthetic noise generator with an (internal) optical receiver. Two control signals are extracted simultaneously from this monitored signal, using the following methods:

- A low-pass filter extracts the dc-current from the monitor signal, and provides a first control signal. This signal is proportional to I_{n0} because it is proportional to the lightwave output power.
- A band-pass filter, cascaded with an envelope detector, provides a second control signal. This signal is proportional to the spectral density S_i if the pass-band of the filter is small, compared to the spectral width B. In practical implementations, the use of a high-pass filter will produce similar results, if the cut-off frequency of the monitor receiver is significantly lower than the spectral width B.

A first control loop decreases the laser bias current when the first control signal increases. This stabilizes the lightwave output power, and makes the setup insensitive to drift in laser power, laser temperature and coupling losses. Multiplication or addition of this signal with the laser bias current will fulfill these requirements.
A second control loop increases the magnitude of the (periodic) modulation signal when the second control signal increases. This stabilizes the spectral density S_i and makes it insensitive to polarization variations in the interfero meter and other drift causes. It requires a controlled attenuator, a controlled amplifier or a multiplier.
Both loops are adequate to minimize drift in a synthetic noise generator, and make stabilization of the individual components superfluous.

9.2.4. Statistical analysis of synthetic noise

Natural noise sources commonly generate Gaussian distributed noise. Simple detection techniques, without true rms-detection, take advantage of this property for instance by estimating the noise rms-value from the detected average top level. The statistical distribution of synthetic noise is significantly different from a Gaussian distribution, and this result in detection errors when inadequate detection techniques are used. In this subsection we discuss the differences in statistical distribution.
The laser beam and the delayed laser beam are both modulated in frequency. The differential frequency, which is related to the differential phase $\Delta\alpha(t)$, is down-converted in the PIN diode, and forms the ac-part $i_n(t)$ of the photo current $I_n(t)$. This current has the following general form: $I_n(t) = I_{n0} \cdot (1 + \cos(\Delta\alpha(t))) = I_{n0} + i_n(t)$.
Since the phase of the laser beam is modulated with a periodic and a random signal, the differential phase is modulated too. In a well-designed synthetic noise generator, the differential delay and the modulation depth is large enough to make $(\Delta\alpha)_{rms} \gg \pi$. As a result, the photo current $I_n(t)$ changes rapidly and at random, and varies from zero to twice the mean photo current I_{n0}.
Figure 9.18 shows a simulated oscilloscope view of the photo current $I_n(t)$. The upper trace has a random appearance, however it has well-defined upper and lower magnitude limits. The lower trace is natural noise and has no limits at all. The difference in appearance demonstrates that the probability distribution of synthetic noise differs significantly from that of natural noise, which is usually Gaussian (normal)-distributed.

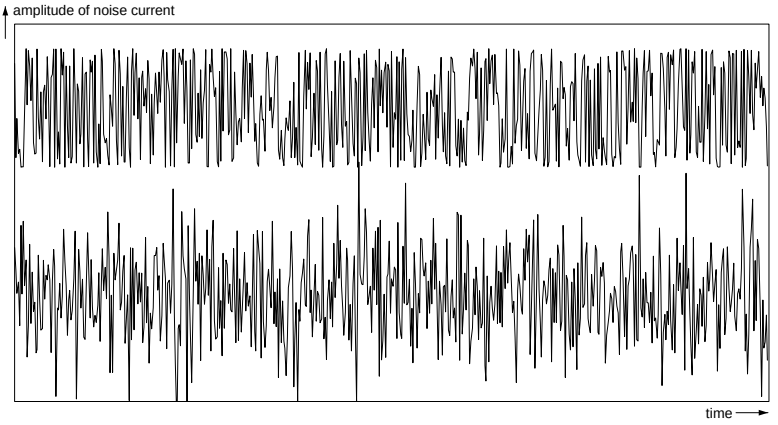

Fig 9.18 *Simulated oscilloscope view of synthetic noise (upper trace) and natural noise (lower trace). The rms-values of both noisy signals are equal. Synthetic noise has a random appearance, however with well-defined upper and lower magnitude limits. This property does not hold for natural noise.*
The upper trace is representative provided that the noise generator operates far above the incoherence threshold (see section 9.3.2). This holds for sinusoidal as well as triangular modulation; with or without noise injection.

When the rms-magnitude of $\Delta\alpha$ is large, then the magnitude distribution of $\Delta\alpha$ is irrelevant for the magnitude distribution of $\cos(\Delta\alpha)$. This is because the function $\cos(\Delta\alpha)$ wraps the results in 2π intervals, and causes the signal $\varphi=\arccos(\cos(\Delta\alpha))$ to be a random signal with near uniform-distribution. This makes the probability distribution proportional to $p(x)=(1/\pi)/\sqrt{a^2-x^2}$, for $|x/a|<1$, a distribution that is named *trigonometric*-distribution in this text. Figure 9.19 shows the trigonometric-distribution of synthetic noise, in combination with the Gaussian-distribution of natural noise.

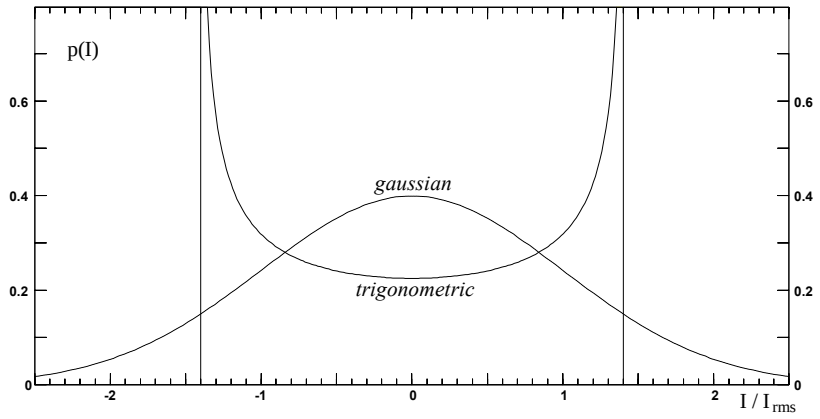

Fig 9.19 *Probability distribution function of synthetic noise, normalized to its rms-value. The rms-value is 70% of the maximum ac-value (=1/Ö2). The function is compared to that of Gaussian distributed noise, with equivalent rms-value.*

Figure 9.19 shows that the difference between trigonometric-distributed noise and Gaussian-distributed noise is significant. This aspect is important for precision calibration measurements on synthetic noise with calibrated noise standards.
Both a *linear* selective voltmeter and a *true-rms* detector are required for correct noise measurement. Nevertheless, many instruments that are specialized for this purpose do not fulfill both requirements. This effect limits their accuracy, which is discussed below.

rms-conversion uncertainty
Noise detection with an envelope detector, in stead of a true-rms detector, will cause erroneous results. Variation of the type of amplitude distribution, with conservation of spectral density, will cause a variation in read-out.
Some commonly used instruments, that are specialized for noise measurement, are sensitive to this type of variations. To quantify this sensitivity, we compared Gaussian-distributed noise of a standard noise source (HP346c) with trigonometric-distributed noise of the synthetic noise source, by using an HP8970a Noise Figure meter. The magnitude of the synthetic noise source was adjusted to facilitate two noise signals with equal spectral density. An internal envelope detector (instrument display) as well as an external true-rms detector (HP8481a power sensor, via 20 MHz IF-output) were used to make this comparison. Inequalities up to 0.2 dB were indicated by the rms-detector, for equal indication with the envelope detector.
As a result, the uncertainty in the rms-conversion factor decreases the overall measurement accuracy when the statistical properties of noise vary. This limits the performance of commonly used noise figure meters and spectrum analyzers

log-compression uncertainty
Noise detection with *logarithmic* selective voltmeters, in stead of *linear* selective voltmeters, will also cause erroneous results. This applies to most spectrum analyzers.

Logarithmic amplifiers do not preserve the statistical distribution of noisy signals, because the higher noise values are not amplified as much as the lower values. This causes a systematic error, due to the difference in instrument sensitivity between periodic and random signals, which requires a correction.
The noise marker of a spectrum analyzer is corrected for this effect, a correction that is optimized for Gaussian distributed noise. A log-correction of about 1.45 dB is required [804] when envelope detection and video filtering are used. Note, that this factor is irrespective to an additional rms-correction factor of 1.05 dB that is required [804] for noise detection with an envelope detector that is calibrated for rms-indication of sinus waves.
As a result, the uncertainty in the log-correction factor degrades the overall measurement accuracy when the statistical properties of noise vary. This is an additional performance limitation of commonly used spectrum analyzers, which does not hold for the above mentioned noise figure meter. In practical situations the total uncertainty of most spectrum analyzers is higher than the rms-conversion uncertainty and the log-compression uncertainty, which makes these uncertainties usually of minor importance.

9.2.5. Conclusions

In conclusion, we analyzed the spectral properties of the synthetic noise generator and demonstrated spectral ripple effects in case of insufficient incoherence. We discussed that a solution with long differential delay may fulfill the incoherence requirements, however excludes the use of multi section lasers.
We proposed a superior alternative, using injection of electrical noise, and analyzed various aspects of this injection. We demonstrated that injection with pink noise, filtered above the modulation frequency of the setup, provides optimal smoothing of the spectral ripple. Further we demonstrated that triangular modulation, in stead of sinusoidal modulation, improves the usable portion of the noise bandwidth. Up to 50% of the spectral width B is applicable for noise measurements.
We demonstrated the high efficiency of synthetic noise generation. Up to 70% of the generated power is available as noise. The spectral width user defined, which facilitates the generation of very high noise levels. Synthetic noise is associated with very low (parasitic) dc-currents. This may be crucial for noise measurements on dedicated low-noise lightwave receivers.
For independent stabilization of optical power and spectral intensity we proposed an new dual loop method. We analyzed the statistical properties of synthetic noise, and discussed the implications of the difference between natural noise and synthetic noise.

9.3. Theoretical analysis of synthetic noise generation

The previous section analyzed many aspects of synthetic noise generation, from a practical point of view. It elucidated these aspects with the help of various simulation results, without discussing the underlying mathematics.
This section will focus on adequate mathematical models of synthetic noise generation, and provides the theory and formulae for the simulated results in the previous section.

9.3.1. Time domain analysis of the synthetic noise signal

A synthetic noise generator is essentially a lightwave oscillator, modulated in frequency. There are two FM modulation inputs, one for a periodic modulation signal I(t) and another for a random signal J(t). A third input for intensity modulation (IM) is required for controlling laser power.
Figure 9.20 shows an adequate calculation model of a synthetic noise generator, in which the FM modulation is represented by an integrator and a phase modulator. The light beams in both interferometer branches are assumed to be equally polarized.

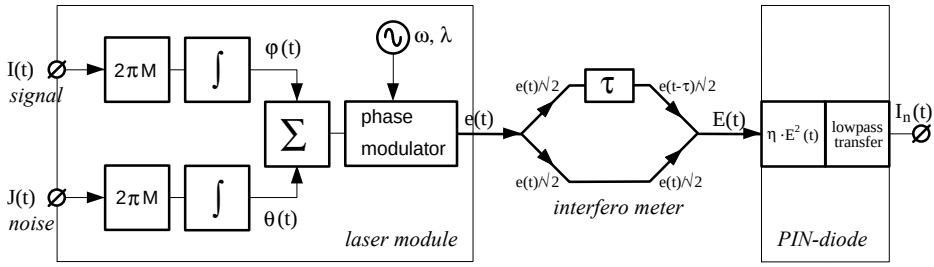

Fig 9.20 *An adequate calculation model of the lightwave synthetic noise generator. I(t) represents the periodical modulation current and J(t) the combination of externally injected noise and internal parasitic noise. Both currents equally affect the laser frequency, however, this model isolates I(t) from J(t) to distinct* j *(t) from* q*(t).*

Variation of the laser bias current yields a variation of lightwave intensity (IM) as well as the lightwave frequency (FM). Nevertheless, our analysis leaves all parasitic intensity modulation effects out of consideration. This is allowed because:

- The combination of interfero meter and PIN diode makes the setup highly sensitive to lightwave FM signals and in practical situations the detected FM signal dominates the parasitic IM signal. This holds for our experimental setup with a DFB laser, and even more when multi section lasers are used. Multi section lasers have separated inputs for IM and FM modulation, while the modulation of DFB lasers is restricted to variation of their bias current.
- Laser intensity noise (RIN) is an example of parasitic IM effects. The calculation examples in section 9.2.3 and 9.3.2 illustrate that synthetic noise dominates the intensity noise (say 40 dB higher).

- Further, parasitic IM components in the photo diode response spectrum are suppressed when their frequency equals an odd multiple of $1/(2\tau)$. This is discussed in section 9.1 when selecting of the optimal delay time τ. When delay time and periodical modulation frequency are optimally matched, then all odd harmonics are suppressed.

As a result, IM modulation effects are of minor importance for the generation of synthetic noise.

The field strength of the modulated lightwave signal is e(t), and this field is split, delayed and combined to the field strength E(t). This signal is proportional to the differential field $e(t)–e(t–\tau)$, and generates a photo current $I_n(t)$ in a PIN diode. This current is the synthetic noise current.
In this subsection we will derive the relation between synthetic noise $I_n(t)$ and the two modulation signals I(t) and J(t). Let $\varphi(t)$ and $\theta(t)$ be the modulation phase at the input of the phase modulator, and let $\Delta\varphi(t,\tau)$ and $\Delta\theta(t,\tau)$ be their differential values with interval τ, then they are as follows related to the modulation signals I(t) and J(t):

$$\varphi(t) \stackrel{\text{def}}{=} 2\pi\cdot M\cdot\int_{-\infty}^{t} I(t)\cdot dt \qquad = \textit{(periodic)}$$

$$\theta(t) \stackrel{\text{def}}{=} 2\pi\cdot M\cdot\int_{-\infty}^{t} J(t)\cdot dt \qquad = \textit{(random)}$$

$$\Delta\varphi(t,\tau) \stackrel{\text{def}}{=} \varphi(t)–\varphi(t–\tau) = 2\pi\cdot M\cdot\int_{t-\tau}^{t} I(t)\cdot dt = 2\pi\cdot M\cdot\int_{-\infty}^{t} \{I(t)–I(t+\tau)\}\cdot dt$$

$$\Delta\theta(t,\tau) \stackrel{\text{def}}{=} \theta(t)–\theta(t–\tau) = 2\pi\cdot M\cdot\int_{t-\tau}^{t} J(t)\cdot dt = 2\pi\cdot M\cdot\int_{-\infty}^{t} \{J(t)–J(t+\tau)\}\cdot dt$$

Let ω_0 be a constant lightwave frequency ($\omega_0\cdot=2\pi\cdot c/\lambda$) that is generated in the ideal lightwave oscillator. Let ω be the momentaneous frequency of the laser output signal. This frequency value ω is fluctuating due to spontaneous emission (phase noise) and thermal drift. The model of figure 9.20 represents all these fluctuations by an integral part of the noise source J(t). This representation facilitates the use of an initial *lightwave* phase ϕ_0 of the unmodulated laser at t=0.
The lightwave signal is divided into two beams in the interfero meter. Let ΔL be the difference in fiber length between the two branches of the interfero meter, then the associated delay ($\tau=\Delta L/c$) results in a phase difference $\Delta\alpha(t,\tau)$ between the two beams when are combined. This differential phase is as follows related to the previous quantities:

$$\alpha_r \stackrel{\text{def}}{=} \phi_0+\omega_0\cdot t+\varphi(t)+\theta(t) \qquad = \textit{reference phase}$$

$$\alpha_d \stackrel{\text{def}}{=} \phi_0+\omega_0\cdot(t–\tau)+\varphi(t–\tau)+\theta(t–\tau) \qquad = \textit{delayed phase}$$

$$\alpha_\tau \stackrel{\text{def}}{=} (\omega_0\cdot\tau \oplus 2\pi) = 2\pi\cdot(\Delta l/\lambda \oplus 1) \qquad = \textit{offset phase}$$

$$\Delta\alpha \stackrel{\text{def}}{=} \alpha_\tau + \Delta\varphi(t,\tau) + \Delta\theta(t,\tau) = (\alpha_r – \alpha_d) + k\cdot 2\pi \qquad = \textit{differential phase}$$

In these expressions, the operation $(x\oplus y)$ denotes the modulo operation that returns the remainder of the division of (x/y) with an integer result. The current $I_n(t)$, that responds in the photo diode from illumination with the lightwave field strength E(t), is now derived as follows:

$$\begin{aligned} e(t) &= E_0 \cdot \cos(\phi_0 + \omega_0 \cdot t + \varphi(t) + \theta(t)) \\ &= E_0 \cdot \cos(\alpha_r) \end{aligned}$$

$$\begin{aligned} E^2(t) &= (\tfrac{1}{2} \cdot e(t) + \tfrac{1}{2} \cdot e(t-\tau))^2 \\ &= (\tfrac{1}{2} \cdot E_0)^2 \cdot \{\cos(\alpha_r) + \cos(\alpha_d)\}^2 \\ &= \tfrac{1}{4} \cdot E_0^2 \cdot \{\cos^2(\alpha_r) + 2 \cdot \cos(\alpha_r) \cdot \cos(\alpha_d) + \cos(\alpha_d)^2\} \\ &= \tfrac{1}{4} \cdot E_0^2 \cdot \{\tfrac{1}{2} + \tfrac{1}{2} \cdot \cos(2\alpha_r) + \cos(\alpha_r + \alpha_d) + \cos(\alpha_r - \alpha_d) + \tfrac{1}{2} + \tfrac{1}{2} \cdot \cos(2 \cdot \alpha_d)\} \\ &= \tfrac{1}{4} \cdot E_0^2 \cdot \{1 + \cos(\alpha_r - \alpha_d) + \cos(\alpha_r + \alpha_d) + \tfrac{1}{2} \cdot \cos(2\alpha_r) + \tfrac{1}{2} \cdot \cos(2 \cdot \alpha_d)\} \end{aligned}$$

$$\begin{aligned} I_n(t) &= (\tfrac{1}{4} \cdot \eta E_0^2) \cdot \{1 + \cos(\alpha_r - \alpha_d)\} \quad + \textit{ Currents at Lightwave Frequencies} \\ &= (\tfrac{1}{4} \cdot \eta E_0^2) \cdot \{1 + \cos(\omega_0 \cdot \tau + \Delta\varphi(t,\tau) + \Delta\theta(t,\tau))\} \\ &= (\tfrac{1}{4} \cdot \eta E_0^2) \cdot \{1 + \cos(\omega_0 \cdot \tau \oplus 2\pi) + \Delta\varphi(t,\tau) + \Delta\theta(t,\tau))\} \\ &= (\tfrac{1}{4} \cdot \eta E_0^2) \cdot \{1 + \cos(\alpha_\tau + \Delta\varphi(t,\tau) + \Delta\theta(t,\tau))\} \\ &= (\tfrac{1}{4} \cdot \eta E_0^2) \cdot \{1 + \cos(\Delta\alpha(t,\tau))\} \end{aligned}$$

$$\begin{aligned} I_n(t) &\stackrel{\text{def}}{=} I_{n0} \cdot (\cos(\Delta\alpha(t,\tau)) + 1) \\ i_n(t) &\stackrel{\text{def}}{=} I_{n0} \cdot \cos(\Delta\alpha(t,\tau)) \\ \\ I_{n0} &\stackrel{\text{def}}{=} (\tfrac{1}{4} \cdot \eta E_0^2) \\ \Delta\alpha(t,\tau) &= (\omega_0 \cdot \tau \oplus 2\pi) + 2\pi \cdot M \cdot \int_{t-\tau}^{t} (I(t) + J(t)) \cdot dt \end{aligned}$$

These equations demonstrate that the magnitude of the output signal spans a restricted range, because of the cosine term. The minimum value is zero and the maximum is $2 \cdot I_{n0}$. We used these expressions to simulate the plots in figure 9.18. The simulations were performed with MatLab, using the following steps:

1): $J(t)$ = array with Gaussian distributed random numbers

2): $\Delta\theta(t,\tau) = 2\pi \cdot M \cdot \int_{-\infty}^{t} \{J(t) - J(t+\tau)\} \cdot dt$

3): $I_n(t) \stackrel{\text{def}}{=} I_{n0} \cdot (\cos(\Delta\theta(t,\tau)) + 1)$

Without any modulation, $I(t)=J(t)=0$, or without any differential delay, $\tau=0$, the differential phase $\Delta\alpha$ is zero, which causes the photo current to be maximal.

9.3.2. Incoherence analysis

The interference between the two light beams in the synthetic noise generator causes a variation in the photo current $I_n(0)$, and the associated ac-current $i_n(t)=I_{n0} \cdot \cos(\Delta\alpha)$ represents the synthetic noise. Periodic modulation will result in deterministic variations of $I_n(t)$, and this situation is referred as a coherent interference. Superposition of a random modulation signal will change this into an incoherent interference, which results in random variation of the photo current.

Incoherent interference is essential for synthetic noise generation. Therefore this subsection derives what values are required for the random modulation J(t) and the differential delay time τ, to perform adequate incoherent interference. It will be demonstrated that this demand is equivalent with the restriction that the differential delay τ must exceed the coherence time τ_c of the laser.

Definition of incoherence threshold

The differential phase $\Delta\alpha$ is the superposition of periodic variations $\Delta\varphi(t,\tau)$, random fluctuations $\Delta\theta(t,\tau)$, and an offset value. The magnitude of these random fluctuations are indicative for the deviation from pure coherent interference, and we define:

Incoherence	$\stackrel{\text{def}}{=} \Delta\theta_{rms}$
Incoherence threshold:	$\Delta\theta_{rms} \stackrel{\text{def}}{=} \pi$

The incoherence increases with the depth of random modulation, however increases with the differential delay τ. Figure 9.21 illustrates the relation between a logarithmic increase of incoherence and the increase of the random fluctuations in the photo current $I_n(t)$.

The deeper the laser is random modulated, the higher the incoherence will be and the more ac-current is generated. When the incoherence equals the value π, then $\cos(\Delta\theta)$ will fluctuate over the full available span. This special value will be referred in this text as the *incoherence threshold.*

Above incoherence threshold, the interference is wrapped in 2π intervals and the current fluctuations span the full available range. The interference between the two lightwave signals will then fluctuate from perfect extinction to perfect superposition.

Figure 9.21 illustrates that the photo current ranges from zero to $2\cdot I_{n0}$. Far below the incoherence threshold, the mean value I_{n0} of the photo current $I_n(t)$ approaches this maximum value, however far above the incoherence threshold the mean value has been reduced to half the maximum photo current.

Further increase of the differential phase will not increase the ac noise magnitude, because it cannot exceed the value I_{n0}. This makes the total available noise power *independent* of the modulation depth. From this, it is concluded that a well-designed synthetic noise generator must always operate far above the incoherence threshold.

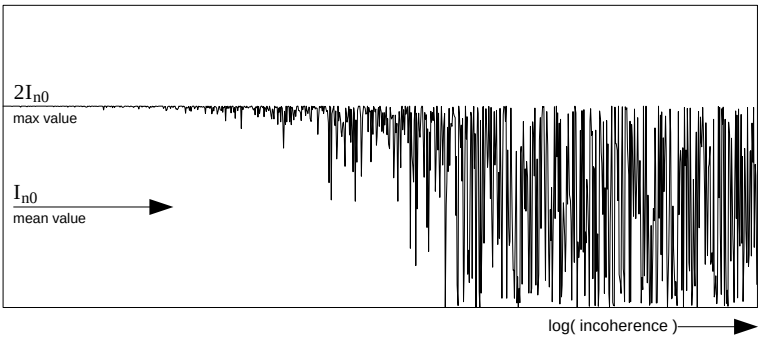

Fig 9.21 *Simulated oscilloscope view of the synthetic noise current $I_n(t)$, in case the random modulation J(t) sweeps from zero to a maximum value. Far above incoherence threshold, the output noise spans the full range, and its mean value I_{n0} has been reduced to half the maximum value.*

Incoherent power analysis

Far above incoherence threshold, the mean of $\cos(\Delta\theta)$ approaches to zero, and facilitates a simple relation between rms-magnitude of the ac noise current and the mean value of the dc current:

$$(i_{rms})^2 = \left\langle i_n^2(t) \right\rangle_\infty = I_{n0}^2 \cdot \left\langle \cos^2(\Delta\theta) \right\rangle_\infty = I_{n0}^2 \cdot \left\langle \tfrac{1}{2} + \tfrac{1}{2} \cdot \cos(2\cdot\Delta\theta) \right\rangle_\infty$$
$$= I_{n0}^2 \cdot \left\langle \tfrac{1}{2} \right\rangle_\infty$$

$$\boxed{i_{rms} = I_{n0}/\sqrt{2} \quad = \textit{rms magnitude of the noise}} \qquad \textit{far above the incoherence threshold}$$

In a well-designed noise generator, the synthetic noise is equally spread out over a wide frequency band B. This width is defined by the frequency modulation depth of I(t). Since the Parceval identity relates the rms-value to the single-sided spectral density $S_i(f)$ of the noise, we obtain for white noise:

$$(i_{rms})^2 = \left\langle i_n^2(t) \right\rangle_\infty = \int_0^{+\infty} S_i(f) \cdot df \approx S_i(0) \cdot B$$

$$\boxed{S_i(f) \approx \left(I_{n0}/\sqrt{2B} \right)^2 \quad \textit{= spectral power density}} \qquad \textit{far above the incoherence threshold}$$

The ratio between spectral density and dc photo current is an important characteristic figure of the synthetic noise source, since it enables the specification of noise at multiple noise levels. It is similar to the definition of laser RIN that is commonly specified in dB/Hz using $10 \cdot \log_{10}(\mu^2)$:

$$\boxed{\mu \stackrel{\text{def}}{=} (\sqrt{S_i})/I_{n0} \approx 1/\sqrt{(2\cdot B)} \quad \textit{= noise-current ratio}} \qquad \textit{far above the incoherence threshold}$$

These formulae demonstrate the validation of conclusions in section 9.2.3, and the observation in section 9.1.2 that the intensity spectrum is reciprocal with the modulation current.

Incoherence sensitivity to differential delay and noise injection

The incoherence $\Delta\theta_{rms}$ increases with the magnitude of the injected noise current J(t) and with the differential delay time τ. Since this is an important aspect of a well-designed synthetic noise generator we calculate the relation between rms-magnitude of the differential phase fluctuation $\Delta\theta$ and of the injected noise current J(t).

Using the Parceval identities, to obtain the rms-magnitude of $\Delta\theta(t,\tau)$ from its single sided intensity spectrum $S_{\Delta\theta}(f)$, we get:

$$(\Delta\theta_{rms})^2 = \left\langle |\Delta\theta(t,\tau)|^2 \right\rangle_{\infty} = \int_0^{+\infty} S_{\Delta\theta}(f)\cdot df = \int_0^{+\infty} \boldsymbol{S}\{\Delta\theta(t,\tau)\}\cdot df$$

using $\Delta\theta(t,\tau) = 2\pi\cdot M\cdot\int_{-\infty}^{t}\{J(t)-J(t+\tau)\}\cdot dt$ *we obtain:*

$$(\Delta\theta_{rms})^2 = (2\pi\cdot M)^2 \cdot \int_0^{+\infty} \boldsymbol{S}\left\{ \int_{-\infty}^{t}\{J(t)-J(t+\tau)\}\cdot dt \right\} \cdot df$$

$$(\Delta\theta_{rms})^2 = (2\pi\cdot M)^2 \cdot \int_0^{+\infty} \left|\frac{1}{j\omega}\right|^2 \cdot \boldsymbol{S}\{J(t)-J(t+\tau)\} \cdot df$$

$$(\Delta\theta_{rms})^2 = (2\pi\cdot M)^2 \cdot \int_0^{+\infty} \left|\frac{1-\exp(j\omega\tau)}{j\omega}\right|^2 \cdot \boldsymbol{S}\{J(t)\} \cdot df$$

After some trigonometric manipulations and the use of the shortcut: sinc(x)=sin(πx)/(πx), we obtain:

$$(\Delta\theta_{rms})^2 = (2\pi\cdot M)^2 \cdot \int_0^{+\infty} \tau^2 \cdot \mathrm{sinc}^2(f\tau) \cdot \boldsymbol{S}\{J(t)\} \cdot df$$

$$\Delta\theta_{rms} = (2\pi\cdot M\cdot\tau)\cdot\sqrt{\int_0^{+\infty} \mathrm{sinc}^2(f\tau)\cdot S_J(f)\cdot df} \qquad = \textit{Incoherence}$$

This expression demonstrates that the incoherence increases with the rms-magnitude of J(t) and the differential delay time τ. Further simplification of the above expression is feasible for two extreme situations: in case of pink noise and of white noise injection.

- Pink noise is defined as noise of which the intensity spectrum S_J decreases with increasing frequency. This facilitates the approximation $\mathrm{sinc}^2(f\tau)\approx 1$ for all frequencies below $f=1/(2\tau)$, and the approximation of $S_J=0$ above this limit. Note, that the corner frequency $1/(2\tau)$ equals the modulation frequency f_m, in a well-designed synthetic noise source.
- White noise is defined as noise of which the intensity spectrum S_J is frequency independent over a sufficient wide frequency interval. This makes $S_J(f)= S_J(0)$ for all frequencies where $\mathrm{sinc}^2(f\tau)$ is significant.

Shot noise is an example of white noise, and is indicative for the minimum injected noise. It originates from the laser bias current I_{bias}, and has $S=2q_0\cdot I_{bias}$ as spectral density. Note that a practical semiconductor laser suffers from spontaneous emission, which may increase this minimum value significantly.

Filtered noise is an example of pink noise, if the corner frequency of the low-pass filter is significantly lower than the modulation frequency.

In the two restricted situations, the expression for the incoherence reduces to:

$$[\Delta\theta_{rms}]_{pink} \approx (2\pi\cdot M\cdot\tau)\cdot\sqrt{\mathrm{sinc}^2(0)\cdot\int_0^{+\infty} S_J(f)\cdot df}$$
$$[\Delta\theta_{rms}]_{white} \approx (2\pi\cdot M\cdot\tau)\cdot\sqrt{S_J(0)\cdot\int_0^{+\infty} \mathrm{sinc}^2(f\tau)\cdot df}$$

Using formula 15.36 from the Mathematical handbook [911] *for the integral of a sinc-function, we obtain:*

$$[\Delta\theta_{rms}]_{pink} \approx (2\pi\cdot M\cdot\tau)\cdot\sqrt{1\cdot\langle|J(t)|^2\rangle_\infty}$$
$$[\Delta\theta_{rms}]_{white} \approx (2\pi\cdot M\cdot\tau)\cdot\sqrt{S_J(0)/(2\cdot\tau)}$$

In the special case that all white noise originates from the shot noise of a dc-current I_{bias}, we may substitute:
$S_J(0) = 2\,q_0\,I_{bias}$

pink noise:	$\Delta\theta_{rms}$	$\approx$	$2\pi\cdot M\cdot\tau\cdot J_{rms}$
white noise:	$\Delta\theta_{rms}$	$\approx$	$2\pi\cdot M\sqrt{\tfrac{1}{2}\tau\cdot S_{J0}}$
shot noise:	$\Delta\theta_{rms}$	$\approx$	$2\pi\cdot M\cdot\sqrt{\tau\cdot q_0\cdot I_{bias}}$

These expressions demonstrate that the incoherence is linear proportional to the magnitude of the injected noise J(t). The sensitivity to noise injection is affected by the differential delay time τ of the interfero meter.

Incoherence condition

In a well-designed synthetic noise generator, the modulation frequency f_m is optimally matched to the differential delay τ of the interfero meter, caused by differential length Δ L. This means that $f_m = 1/(2\tau) = c/(2\cdot\Delta L)$, in which c is speed of light in the used fiber. Operation above incoherence threshold set additional prior conditions to the injected noise J(t) and the modulation frequency f_m of the modulation signal I(t).
The relation between incoherence, the random modulation magnitude and the differential delay is described before. As a result, operation above incoherence threshold requires one of the following conditions:

LF pink noise:	$f_m = 1/(2\tau) = c/(2\cdot\Delta L) < M\cdot J_{rms}$
white noise:	$f_m = 1/(2\tau) = c/(2\cdot\Delta L) < M^2\cdot S_J(0)$
shot noise:	$f_m = 1/(2\tau) = c/(2\cdot\Delta L) < 2M^2\cdot q_0\cdot I_{bias}$

These expressions demonstrate that compensation of a shortage in differential delay requires an abundance in noise modulation to perform incoherent operation.

A rough estimation of the laser linewidth is $\Delta f \approx 2 \cdot M \cdot J_{rms}$. Using this approximation for substitution in the incoherence condition for white noise modulation, then this condition reduces to $f_m = (1/2\tau) < (\Delta f)/2$. Since the coherence time t_c is related to this width by $\tau_c = \Delta f$, the incoherence condition is equivalent with the condition that the differential delay must exceed the coherence length.
This validates one of the conclusions of the Wang experiment [907] that the delay τ in the homodyne set-up should be larger than the coherence time of the laser diode.

practical calculation example
The shot noise condition is mainly a hypothetical condition since other random effects, such as spontaneous emission, dominate in practical semiconductor lasers. This can be concluded from the RIN (relative intensity noise) that is specified for commercially available laser diodes.
RIN is defined for a specific laser bias current I_{bias} when the laser under test illuminates a photo diode. Let S_i be the detected intensity spectrum of a laser in *excess* to the receiver noise and the shot noise of the generated photo current I_{photo}. Now RIN is defined as the ratio $\mu^2 = S_i/(I_{dc})^2$, and is commonly specified in [dB/Hz] using $10 \cdot \log_{10}(\mu^2)$.
Further, let R be the current responsivity of the setup, being defined as $R = I_{photo}/I_{bias}$. The relation between the laser intensity noise S_i (at the photo diode side) and the equivalent noise S_J (at the laser side) 'generating' this intensity noise is as follows:

$$\mu^2 = \frac{S_i}{(I_{photo})^2} = \frac{R^2 \cdot S_J}{(R \cdot I_{bias})^2} = \frac{S_J}{(I_{bias})^2} \stackrel{\text{def}}{=} \frac{\alpha \cdot (2q_0 \cdot I_{bias})}{(I_{bias})^2} = \alpha \cdot \left(\frac{2q_0}{I_{bias}} \right)$$

In these expressions is a *an enhancement factor that indicates how much the spontaneous emission dominates the shot noise of the laser bias current.*

In the hypothetical case that α=1, than the RIN level would have been –172 dB/Hz for 50 mA laser bias current. Usually, the specified RIN level is 20 dB higher which yields that α=100.

To quantify the incoherence condition for the above laser example, assume that the FM sensitivity of the laser module is M = 300 MHz/mA and a bias current of I_{bias}=50mA. On one hand, this generator requires at least J_{rms}=33μA of pink noise when a modulation frequency of f_m=10MHz ($\Delta L \approx 10$ m) is optimal and when all noise is injected as pink noise. On the other hand, this generator requires at most an optimal modulation frequency of f_m=140 kHz ($\Delta L \approx 700$ m) when all noise originates from laser intensity noise (α=100 times the shot noise of 50 mA bias current).

9.3.3. Spectral analysis far above incoherence threshold

The time domain analysis of subsection 9.3.1 requires detailed information on the phase of the lightwave signal, with respect to t=0. This phase information is available for the periodic modulation signal I(t), however the noise signal J(t) is random and the internal part of J(t) is not available for measurement.
A well-designed synthetic noise generator operates above incoherence threshold, and one of the consequences is that the statistical properties and the intensity spectrum of the synthetic noise are not affected by an arbitrary phase offset of the lightwave signal.
This subsection demonstrates that operation above incoherence threshold yields a significant simplification of spectral calculus. Further it applies this simplification to spectral analysis of the full synthetic spectrum.

Mean values above incoherence threshold

When $\Delta\theta(t)$ is a random signal with zero mean, and ϕ_0 is a constant phase offset, then the modulated signal $\cos(\Delta\theta(t)+\phi_0)$ is random too. This signal has a mean value that depends on the phase offset term ϕ_0. This dependency is not linear and exists for small modulation signals only. Far above or far below the incoherence threshold this dependency is approximated by:

$\langle\cos(\Delta\theta(t)+\phi_0)\rangle_\infty \approx \cos(\phi_0)$ *for near coherent situations, when* $\Delta\theta_{rms} \ll \pi$
$\langle\cos(\Delta\theta(t)+\phi_0)\rangle_\infty \approx 0$ *for incoherent situations, when* $\Delta\theta_{rms} \gg \pi$

Operation above incoherence threshold was defined in section 9.3.2 and means that $\Delta\theta_{rms} > \pi$. As a result, the differential phase $\Delta\theta$ fluctuates over more than a 2π span. Therefore, the constant phase offset ϕ_0 will hardly affect the statistical (and spectral) properties of the modulated signal. For an arbitrary phase offset ϕ_0, an arbitrary delay time t_0, and arbitrary random values $\Delta\theta(t)$ with *sufficient* magnitude (far above the incoherence threshold), this results in:

$$\langle\sin(\Delta\theta(t))\rangle_\infty = 0 \qquad \langle\cos(\Delta\theta(t))\rangle_\infty = 0$$
$$\langle\sin(\Delta\theta(t)+\phi_0)\rangle_\infty = 0 \qquad \langle\cos(\Delta\theta(t)+\phi_0)\rangle_\infty = 0$$
$$\Big\langle\sin\big(\Delta\theta(t)+\Delta\theta(t+t_0)\big)\Big\rangle_\infty = 0 \qquad \Big\langle\cos\big(\Delta\theta(t)+\Delta\theta(t+t_0)\big)\Big\rangle_\infty = 0$$
$$\Big\langle\sin\big(\Delta\theta(t)-\Delta\theta(t+t_0)\big)\Big\rangle_\infty = 0 \qquad \Big\langle\cos\big(\Delta\theta(t)-\Delta\theta(t+t_0)\big)\Big\rangle_\infty = \delta$$

if $|t_0| \gg 0$ ***then*** $\delta \to 0$
if $|t_0| \to 0$ ***then*** $\delta \to 1$

As a result, most of these examples have zero mean, with an exception for the cosine differential case. It approaches to the value 1, in the limit that the differential delay approaches to zero.

Intensity spectra far above incoherence threshold

The calculation of random modulated FM spectra is simplified when the modulation exceeds the incoherence threshold significantly. This is because a change in phase offset will not result in a change of the intensity spectrum.

Let the operators $\boldsymbol{S}\{\}$ and $\mathbf{j}_c\{\}$ denote the transformation from the time domain to the *single sided intensity spectrum* and the *continuous Fourier spectrum* respectively (see section 7.1), and let $f^*(t)$ denote the complex conjugate of the function $f(t)$, then spectral calculus far above incoherence threshold yields for an arbitrary random function $\theta(t)$:

$$\begin{aligned}
\boldsymbol{S}\{\cos(\theta(t))\} &= 2\cdot\mathbf{j}_c\{\langle\cos(\theta(t))\cdot\cos^*(\theta(t+\tau))\rangle_\infty\} \\
&= 2\cdot\mathbf{j}_c\{\langle\tfrac{1}{2}\cdot\cos(\theta(t)-\theta(t+\tau)) + \tfrac{1}{2}\cdot\cos(\theta(t)+\theta(t+\tau))\rangle_\infty\} \\
&= \mathbf{j}_c\{\langle\cos(\theta(t)-\theta(t+\tau))\rangle_\infty\} + \mathbf{j}_c\{\langle\cos(\theta(t)+\theta(t+\tau))\rangle_\infty\} \\
&= \mathbf{j}_c\{\langle\cos(\theta(t)-\theta(t+\tau))\rangle_\infty\} \\
&= \mathbf{j}_c\{\langle\exp(j\cdot\theta(t)-j\cdot\theta(t+\tau)) - j\cdot\sin(\theta(t)-\theta(t+\tau))\rangle_\infty\} \\
&= \mathbf{j}_c\{\langle\exp(j\cdot\theta(t)-j\cdot\theta(t+\tau))\rangle_\infty\} \\
&= \mathbf{j}_c\{\langle\exp(j\cdot\theta(t))\cdot\exp^*(j\cdot\theta(t+\tau))\rangle_\infty\}
\end{aligned}$$

$$\boxed{\boldsymbol{S}\{\cos(\theta(t))\} = \tfrac{1}{2}\cdot\boldsymbol{S}\{\exp(j\cdot\theta(t))\}}$$

This expression demonstrates that the intensity spectrum of a *real* trigonometric modulation equals the intensity spectrum of a *complex* exponential function. The exponential form has no physical meaning however simplifies spectral calculation of frequency or phase modulated signals.

The intensity spectrum of a trigonometric modulated signal with offset is calculated as follows:

$$\begin{aligned}
\boldsymbol{S}\{\cos(\theta(t)+\delta_0)\} &= \tfrac{1}{2}\cdot\boldsymbol{S}\{\exp(j\cdot\theta(t)+j\cdot\delta_0)\} \\
&= \tfrac{1}{2}\cdot\boldsymbol{S}\{\exp(j\cdot\theta(t))\}\cdot|\exp(j\cdot\delta_0)|^2 \\
&= \tfrac{1}{2}\cdot\boldsymbol{S}\{\exp(j\cdot\theta(t))\}
\end{aligned}$$

$$\boxed{\boldsymbol{S}\{\cos(\theta(t)+\delta_0)\} = \boldsymbol{S}\{\cos(\theta(t))\}}$$

This expression demonstrates that the intensity spectrum of FM-modulated signals is invariant for constant phase shifts, when it is random modulated far above incoherence threshold. Note that this will not hold for variable phase shift.

Intensity spectrum of synthetic noise

The intensity spectrum of the synthetic noise signal is affected by random as well as periodic modulation signals J(t) and I(t). The addition of (periodic) modulation provides an additional phase shift, to increase the spectral width. We define two spectra: $S_h(f)$ and $\overset{\infty}{Q}(n)$.

- The continuous intensity spectrum $S_h(f)$ is associated with the random differential phase $\Delta\theta$ that is caused by the random modulation signal J(t). We will refer to it as the (self) homodyne spectrum.
- The discrete Fourier spectrum $\overset{\infty}{Q}(n)$ is associated with the periodic differential phase $\Delta\varphi$ that is caused by the periodic modulation signal I(t) with period T. We will refer to it as the frame of the synthetic noise spectrum

These spectra are defined as follows:

$$S_h(f) \overset{def}{=} \mathcal{S}\{I_{n0} \cdot \cos(\Delta\theta(t,\tau))\} \quad = \textit{(continuous) intensity base spectrum}$$

$$\overset{\infty}{Q}(n) \overset{def}{=} \mathcal{F}_d\{\exp(j\cdot\Delta\varphi(t,\tau);\ T\} \quad = \textit{(discrete) Fourier line spectrum}$$

The (self) homodyne spectrum $S_b(f)$ is the intensity spectrum of the synthetic noise in the special case that the periodic modulation is switched off.

The frame $\overset{\infty}{Q}(n)$ is a set of Fourier coefficients that is associated with $\Delta\varphi$. It has no direct physical meaning, however we will use it to spit a periodic FM signal in its harmonic components. The Fourier decomposition of $\exp(j\cdot\Delta\varphi)$ with period $T=1/f_m=1/(2\pi\omega_n)$ has the following standard form:

$$\exp(j\cdot\Delta\varphi(t,\tau)) \quad = \sum_{n=-\infty}^{+\infty} \overset{\infty}{Q}_n \cdot \exp(j\cdot n\omega_m t)$$

Using this decomposition, and using the property that trigonometric and exponential modulated random signals yield equivalent intensity spectra, we obtain for the overall synthetic noise spectrum:

$$\begin{aligned}
\mathcal{S}\{i_n(t)\} &= \mathcal{S}\{I_{n0} \cdot \cos(\Delta\alpha)\} \\
&= \mathcal{S}\{I_{n0} \cdot \cos(\alpha_\tau + \Delta\theta(t,\tau) + \Delta\varphi(t,\tau))\} \\
&= \tfrac{1}{2}\cdot(I_{n0})^2 \cdot \mathcal{S}\{\exp(j\cdot\alpha_\tau + j\cdot\Delta\theta(t,\tau) + j\cdot\Delta\varphi(t,\tau))\} \\
&= \tfrac{1}{2}\cdot(I_{n0})^2 \cdot \mathcal{S}\{\exp(j\cdot\alpha_\tau) \cdot \exp(j\cdot\Delta\theta(t,\tau)) \cdot \exp(j\cdot\Delta\varphi(t,\tau))\} \\
&= \tfrac{1}{2}\cdot(I_{n0})^2 \cdot |\exp(j\cdot\alpha_\tau)|^2 \cdot \mathcal{S}\{\exp(j\cdot\Delta\theta(t,\tau)) \cdot \exp(j\cdot\Delta\varphi(t,\tau))\} \\
&= \tfrac{1}{2}\cdot(I_{n0})^2 \cdot 1 \cdot \mathcal{S}\{\exp(j\cdot\Delta\theta(t,\tau)) \cdot \sum \overset{\infty}{Q}_n \cdot \exp(j\cdot n\omega_m t)\} \\
&= \tfrac{1}{2}\cdot(I_{n0})^2 \cdot \sum |\overset{\infty}{Q}_n|^2 \cdot \mathcal{S}\{\exp(j\cdot\Delta\theta(t,\tau)) \cdot \exp(j\cdot n\omega_m t)\}
\end{aligned}$$

$$\boxed{\mathcal{S}\{i_n(t)\} \quad = \sum_{n=-\infty}^{+\infty} |\overset{\infty}{Q}_n|^2 \cdot S_h(f+n\cdot f_m)}$$

These expressions demonstrate that the overall intensity spectrum is the superposition of similar homodyne spectra, centered at equidistant center frequencies. The frame spans the overall synthetic noise spectrum.

All comb lines of the overall synthetic noise spectrum have equal envelope, and this envelope is identical to the shape of this homodyne spectrum. As a result, the frame has

'duplicated' this homodyne spectrum to span the overall synthetic noise spectrum. The contribution to the total spectrum of all these 'duplicated' homodyne spectrum is weighted by the individual frame coefficients $\tilde{\tilde{Q}}_n$.

Simulation of the intensity spectra

The previous expressions are important for simulation purposes. The simulated of the line spectra (frame) were previously shown in the figures 9.5 9.7, 9.8 and 9.9. These simulations were performed in MatLab, following three succeeding steps:

1): $I(t)$ = array with samples of the periodical modulation current

2): $\Delta\varphi(t,\tau) = 2\pi \cdot M \cdot \int_{-\infty}^{t} \{I(t) - I(t+\tau)\} \cdot dt$

3): $\tilde{\tilde{Q}}(n) = \mathcal{F}_d\{\exp(j \cdot \Delta\varphi(t,\tau);\ T\}$

In the first step, the current I(t) was modeled by an array with samples of a single modulation period, for instance a sinusoidal or a triangular function.
In the second step, the differential phase $\Delta\varphi$ was evaluated by substracting two arrays with samples of I(t) and I(t+τ), and then elementwise summated to simulate the integration.
In the third step, the spectral components of $\tilde{\tilde{Q}}(n)$ were extracted from the samples of $\Delta\varphi$ using standard FFT techniques. This approach is applicable for arbitrary modulation currents, and therefore more flexible then an approach with Bessel functions. Moreover, FFT techniques produce the same result with less computational effort.

The homodyne spectrum was made available by measurement (figure 9.15) or by calculation with many random numbers (figure 9.16). The simulation was performed, similarly as described above. The intensity spectrum was evaluated by averaging the square of many FFT samples in a small frequency band.

1): $J(t)$ = array with Gaussian distributed random numbers

2): $\Delta\theta(t,\tau) = 2\pi \cdot M \cdot \int_{-\infty}^{t} \{J(t) - J(t+\tau)\} \cdot dt$

3): $S_h(f) = \mathcal{S}\{I_{n0} \cdot \cos(\Delta\theta(t,\tau))\}$

The major difference is that random numbers were used in stead of a periodic signal, which requires many samples to obtain a smoothed intensity spectrum. A single FFT calculation over $15 \cdot 10^6$ numbers was avoided using 450 individual FFT calculations over 32768 samples. All these intermediate results were combined in a common average.

Power conservation
Using the well-known Parceval identity for spectra, we obtain for the overall homodyne power and overall frame power:

$$\int_0^{+\infty} |S_h(f)|^2 \cdot df = \left\langle \left| I_{n0} \cdot \cos(\Delta\theta(t,\tau)) \right|^2 \right\rangle_\infty = \tfrac{1}{2} \cdot (I_{n0})^2 = (i_{rms})^2$$

$$\sum_{n=-\infty}^{+\infty} \tilde{\tilde{Q}}_n = \left\langle \left| \exp(j \cdot \Delta\varphi(t,\tau)) \right|^2 \right\rangle_\infty = 1$$

$$\int_0^{+\infty} |S_h(f)|^2 \cdot df = (i_{rms})^2$$
$$\sum_{n=-\infty}^{+\infty} \tilde{\tilde{Q}}_n = 1$$

These expressions demonstrate that the frame spreads the homodyne spectrum out over a wide frequency interval, however preserves all available power. The wider the envelope of the frame, the lower the overall spectral density will be.

9.3.4. Statistical analysis far above incoherence threshold

The statistical distribution of synthetic noise differs significantly from the distribution of natural noise. The maximum momentaneous magnitude of pure synthetic noise will never exceed twice the rms-value, while the spikes in natural noise will exceed this value with ease.
Above incoherence threshold the distribution of synthetic noise becomes insensitive for the distribution of the random modulation. This subsection demonstrates that this distribution approaches to a trigonometric distribution, far above the incoherence threshold.

The output signal of a synthetic noise generator has the following general form:

$$I_n(t) = I_{n0} \cdot (\cos(\Delta\alpha(t,\tau)) + 1)$$
$$i_n(t) = I_{n0} \cdot \cos(\Delta\alpha(t,\tau))$$

The differential phase $\Delta\alpha$ is not restricted in magnitude, and may have any statistical distribution and momentaneous magnitude. The wrapped phase $\varepsilon \stackrel{\text{def}}{=} \arccos(\cos(\Delta\alpha))$ is a quantity that is restricted from 0 to π. Modulation with $\Delta\alpha$ or ε will result in equal synthetic noise signals however the distribution function of both phase terms will differ significantly.
The higher the incoherence is, the higher the rms-value of $\Delta\alpha$ will be, and the more ε is wrapped. In the limit, all values between $(0 \le \varepsilon \le \pi)$ have equal statistical performance, which gives ε a uniform distribution. As a result, the statistical distribution of the wrapped phase is $p_\varepsilon(\varepsilon)=1/\pi$ within that interval, and is zero for $(\varepsilon < 0)$ and $(\varepsilon > \pi)$.

Let $i_n(t)$ be a synthetic noise current, and let i_{nx} be an arbitrary constant value within the interval $(-I_{n0} \le i_n \le +I_{n0})$, then $\varepsilon(t)$ and ε_x are the associated wrapped phase terms. The probability that $i_n(t)$ exceeds the value i_{nx} is then as follows:

$$\begin{aligned}\underline{\underline{R}}\{i_n > i_{nx}\} &= \underline{\underline{R}}\{\arccos(i_n/I_{n0}) < \arccos(i_{nx}/I_{n0})\}\\ &= \underline{\underline{R}}\{\varepsilon<\varepsilon_x\}\\ &= 1 - \underline{\underline{R}}\{\varepsilon > \varepsilon_x\}\\ &= 1 - (\varepsilon_x/\pi)\\ &= 1 - \arccos(i_{nx}/I_{n0})/\pi\end{aligned}$$

The distribution function, or probability density, is the derivative of this probability, and is as follows:

$$p_i(i_{nx}) = \frac{\partial}{\partial i_{nx}}\{1 - \arccos(i_{nx}/I_{n0})/\pi\} = \frac{1/\pi}{\sqrt{I_{n0}^2 - i_{nx}^2}}$$

$$p_i(i) = \frac{1/\pi}{\sqrt{2 \cdot i_{rms}^2 - i^2}} \qquad |i| \le i_{rms}\cdot\sqrt{2}$$

This expression demonstrates that synthetic noise has a trigonometric distribution, as was shown in figure 9.19. It differs significantly from Gaussian distributed noise, which has the following well-known form:

$$p_i(i) = \frac{1}{\sqrt{(2\cdot\pi)}\cdot i_{rms}} \cdot \exp\left(-\tfrac{1}{2} \cdot (i/i_{rms})^2\right) \qquad \textit{Gaussian (normal) distribution}$$

The distribution function is a commonly used alternative for spectral calculus to evaluate the mean value or rms-value of noise. It has the following general properties:

$$\underline{\underline{R}}\{I > I_x\} = \int_{-\infty}^{+I_x} p(i) \cdot di \qquad \textit{probability}$$

$$\langle I(t) \rangle_\infty = \int_{-\infty}^{+\infty} p(i) \cdot i \cdot di \qquad \textit{mean value}$$

$$\langle I(t)^2 \rangle_\infty = \int_{-\infty}^{+\infty} p(i) \cdot i^2 \cdot di \qquad \textit{intensity}$$

9.3.5. Conclusions

In conclusion, we developed a general theory for the generation of synthetic noise. We proposed an adequate calculation model and developed a time-domain description for the synthetic noise current. These formulae demonstrate that the magnitude of a synthetic noise current spans a restricted range.

Our theoretical study has resulted in the following concepts and expressions:

- Proposal of a new concept, the *incoherence threshold*. A well-designed synthetic noise generator must always operate far above this threshold.
  Our definition of operation above coherence threshold is equivalent with the condition that the differential delay time of the interferometer must exceed the coherence time of the laser [907]. A shortage in differential delay is fully compensatable with additional noise injection. This addition facilitate operation above incoherence threshold.

- Derivation of expressions for the rms-magnitude, the intensity spectrum S_i and the noise-current ratio μ of synthetic noise currents. The validation of these expressions is restricted to synthetic noise generators operating far above incoherence threshold.
- Derivation of expressions for the incoherence, in case of pink noise and white noise injection. These expressions resulted in conditions to ensure operation above incoherence threshold.
- Derivation of an expression for the overall synthetic noise spectrum. This spectrum is the superposition of many similar homodyne spectra, centered at equidistant center frequencies (comb lines). The frame spans the overall spectrum, and weights the contribution of each comb line to the overall spectrum. These expressions facilitate simulation of the synthetic noise spectrum, for arbitrary modulation currents.
- Evaluated of the probability distribution function of synthetic noise. It is demonstrated that this statistical distribution differs significantly from Gaussian distributed noise.

This theoretical section 9.3 is essential for an analysis as described in section 9.2.